T H E U N I V E R S I T Y O F M I C H I G A N

COLLEGE OF ENGINEERING
Cast Metals Laboratory

Technical Report

EQUILIBRIUM IMMISCIBILITY RELATIONS FOR THE DEVELOPMENT OF MAGNESIUM-FERROSILICON ALLOYS

P. J. Guichelaar
P. K. Trojan
R. A. Flinn

ORA Project 08681

under contract with:

UNION CARBIDE CORPORATION
MINING AND METALS DIVISION
NEW YORK, NEW YORK

administered through:

OFFICE OF RESEARCH ADMINISTRATION ANN ARBOR

January 1969

SUMMARY

Magnesium ferrosilicon alloys have been extensively used for the production of ductile cast iron. However, certain properties of the commercially available alloys have limited their more widespread application. Equilibrium data which would define the characteristic parameters of more efficient alloys have not been available because of experimental difficulties. The purpose of this investigation was therefore to determine the extent of the miscibility gap between iron and magnesium in the iron-magnesium-silicon system and also to determine the magnesium vapor pressure relations within the immiscibility envelope.

Desired bulk compositions were equilibrated in a specially developed crucible under argon pressure to prevent the magnesium from boiling. Samples were taken in situ from the liquid metal layers for chemical analysis.

Magnesium vapor pressure measurements were made using a liquid boiling technique specifically developed for this investigation. The validity of the method was verified by determining the vapor pressure of pure magnesium over a range from 3 atmospheres to 15 atmospheres.

The liquid miscibility gap in the iron-magnesium-silicon system at 2650°F can be categorized into three regions:

1. An initial region where the magnesium solubility in the iron-rich liquid increases from 0.85 percent to 2.5 percent as the silicon content increase from 5.3 percent to 17 percent and where the iron solubility in the magnesium-rich liquid remains almost unchanged at 3.0

percent from zero to 10 percent silicon.

2. A region where the magnesium solubility changes rapidly in the iron-rich phase to 15.2 percent at 34 percent silicon and the iron content of the magnesium correspondingly increases to 21.5 percent at 33 percent silicon.
3. The critical composition region at a total silicon content of 35 to 40 percent where the two miscibility curves meet.

Fourth element additions of cobalt, manganese, carbon, and zirconium had only a minor effect on solubility and vapor pressure relations.

The solubility and vapor pressure relations have important implications for the design of more efficient alloys to produce ductile cast iron. Magnesium-iron-silicon alloys with a low silicon-to-magnesium ratio, a high density, and a reasonable vapor pressure are entirely feasible in view of the results.

TABLE OF CONTENTS

TABLE OF CONTENTS (Concluded)

LIST OF TABLES

LIST OF FIGURES

LIST OF FIGURES (Concluded)

I. INTRODUCTION

Ductile cast iron with its highly desirable spheroidal shaped graphite has become a significant engineering material following its introduction less than twenty years ago. The range of physical properties which can be obtained and the ease with which complex configurations can be cast compare favorably with its relatively low cost. However, the manufacturing technology associated with producing ductile cast iron is still evolving at a fairly rapid rate, reflecting the complex and little understood underlying physical phenomena.

The literature is replete with descriptions of various manufacturing processes which can be used to produce ductile cast iron.[1,2,3] Of these, the majority involve adding magnesium to a molten cast iron bath, either as part of a master alloy or in elemental form. Since the vapor pressure of pure magnesium is over 10 atmospheres at the usual treatment temperatures, the addition of magnesium is generally accompanied by considerable pyrotechnics. This behavior is common even for the most widely used master alloy, magnesium ferrosilicon. For example, when using the popular 10 percent magnesium, 45 percent silicon, 45 percent iron alloy, over 75 percent of the available magnesium can be lost through oxidation and vaporization.[4] The problem is compounded by the comparative low density of the alloy which causes it to rise to the iron bath surface where it can oxidize and vaporize rapidly. The intimate contact between the alloy and the iron bath is therefore lessened when compared to an immersed condition which would favor higher alloy recovery.

This family of nodularizing alloys, the magnesium ferrosilicons, has become commercially dominant chiefly due to its low cost, relative ease of application, and consistent nodularizing quality. Nevertheless, the high silicon contents (40 to 50 percent) and low density (3.5 to 4.0 gm/cc) of the common alloys do not represent the most desirable condition. Present manufacturing practice is limited to these silicon contents since at the temperature range for molten ferrosilicon the magnesium vapor pressure exceeds 1 atmosphere at lower silicon contents. Alloys of higher iron content, lower silicon content, and higher density would be very desirable. However, the magnesium solubility and vapor pressure information necessary to define the manufacturing parameters is not available.

This investigation was therefore undertaken to determine the solubility relationships within the iron-magnesium-silicon ternary system at low silicon contents and to also determine the corresponding magnesium vapor pressures. Additional effects of fourth elements were also investigated to determine if the basic ternary relations could be modified.

II. REVIEW OF THE LITERATURE

The literature pertinent to the equilibrium investigation can be divided into two categories:

A. Available equilibrium information.

B. Theoretical considerations.

A. AVAILABLE EQUILIBRIUM INFORMATION

The major objective of this investigation deals with the equilibrium relationships within the ternary system, magnesium-iron-silicon. However, the boundaries of the ternary are the three distinct binary systems which comprise the limiting conditions for these equilibrium relationships.

Of these three binaries, the system iron-silicon has been thoroughly investigated, both with regard to phase relations and thermodynamic data.[5,6] The strong negative deviation from ideal solution behavior, characteristic of compound formation as present in this system, is indicative of Fe-Si atomic clustering in the liquid state.[7] Similarly, the phase diagram for the magnesium-silicon system shows compound formation and thus the liquid solutions would also be expected to show a negative departure from ideality.[5] Eldridge, et al.,[8] showed the negative deviation in their isopiestic study of the Mg-Si system. The binary system iron-magnesium has not been fully established. The available data indicate that molten magnesium has a very limited solubility for iron.[5] The data of Trojan[9] show a liquid-liquid miscibility gap between carbon-saturated iron and magnesium, with a limited

solubility of magnesium in the iron-rich liquid. Sponseller[10] established immiscibility for a similar system, calcium-iron. Thus, for the iron-magnesium system, it appears that there is a very strong positive departure from the ideal solution behavior.

Very little information is available for the iron-magnesium-silicon ternary system. Zwicker[11] shows what is essentially a crystallization diagram for compositions containing at least 50 percent silicon. This 50 percent silicon limit was imposed by the magnesium vapor pressure which exceeded 1 atmosphere at lower silicon contents. Significantly, the diagram makes no reference to any immiscibility between liquid iron and liquid magnesium in direct contrast to the findings of Trojan.[9]

The results of Trojan indicate a silicon partition factor of 50:1 in favor of the iron-rich phase. Additionally, the magnesium solubility in the iron-rich phase was enhanced by higher silicon contents, but the solubility of iron in the magnesium-rich phase did not appear to increase with higher silicon contents. The results of Sponseller were similar for the effect of silicon which enhanced calcium solubility in pure iron. Therefore, the silicon partition in the iron-magnesium-silicon ternary system should be in favor of the iron-rich phase.

B. THEORETICAL CONSIDERATIONS

Although there have been attempts to mathematically represent the condition of liquid immiscibility in metallic systems, the theories have not yet been developed to the degree where they could serve in place of laboratory techniques. In a recent review paper, Klodt[12] points out that the various pre-

diction theories cannot yet uniquely define the state of immiscibility. With regard to the more complex condition of a ternary system, he indicated that the elementary correlations obtainable showed major inconsistencies when several known systems were compared. The justification for experimental work in this field is therefore apparent.

III. EXPERIMENTAL METHOD

In the present investigation, the effect of silicon on the shape of the miscibility gap between iron and magnesium was determined. Additionally, the magnesium vapor pressure was determined for compositions lying on the miscibility curve. The effect of additions of certain fourth elements on the solubility relationships and the magnesium vapor pressure was also measured. The experimental method developed to make these determinations is described under the following divisions:

A. Experimental design.

B. Experimental equipment.

C. Conduct of a typical experiment.

D. Interpretation of experimental data.

A. EXPERIMENTAL DESIGN

1. Solubility Study

The particular technique used to study the liquid immiscibility required equilibration of a two-phase melt at a desired temperature and bulk composition under argon pressure. If two-liquid miscibility prevails for these conditions, samples can be removed from each of the liquid layers for chemical analyses.

Gibb's phase rule is particularly useful for analysis of a system of this type.[13] It can be stated in a generalized form as

$$V = C - P + 2$$

where V = variance or degrees of freedom

C = the number of components

P = the number of phases in equilibrium

and 2 refers to the phase-rule variables of temperature and pressure.

For the situation where iron, magnesium, and silicon are equilibrated under an argon atmosphere,

C = 4 (iron, magnesium, silicon, argon)

P = 3 (iron-rich liquid, magnesium-rich liquid and vapor phase).

Thus, the variance becomes

$$V = 4 - 3 + 2 = 3 \quad .$$

When the temperature is held constant and the pressure is maintained constant at some value above the boiling pressure of magnesium, the variance is reduced by 2. Therefore, the variance becomes,

$$V = 1 \quad .$$

This implies that for a fixed silicon addition, the one degree of freedom has been utilized and the system becomes unique or completely defined. (All other phase variables such as compositions of the liquid phases and vapor phase are fixed.) Correspondingly, if the composition of one of the equilibrium liquid phases is known, the composition of the other liquid phase must be fixed and related to the first liquid in a unique manner. With the conventional

representation for ternary equilibrium systems, the relationship would be a unique two-phase tie-line. Therefore, by appropriate changes in the bulk silicon composition over a series of experiments at constant temperature and pressure, the profile of the miscibility gap is traced out and the corresponding tie lines define the two-phase liquid equilibria.

The inclusion of argon gas as a phase-rule component does not imply that it represents a solubility parameter. The argon is necessary to establish a system pressure to prevent the magnesium from boiling away. Argon, being an inert gas, does not have a measurable solubility in liquid metals.[14] The effect of this argon gas pressure on the liquid solubility relationships is negligible.[15] However, the gaseous phase is composed of both argon and magnesium vapor and therefore, the presence of argon gas must be considered in the phase rule analysis.

In an experiment where the effect of an additional alloying element is to be determined, (Fe-Si-Mg-A-X), the phase rule analysis yields:

$$V = C - P + 2 = 5 - 3 + 2 = 4$$

As before, at constant temperature and pressure,

$$V = 2 \quad .$$

To uniquely define this system, two variables must be determined or fixed. For convenience, the silicon content and the alloying element (X) content of the overall mixture can be specified. However, the convenient graphical representation of the ternary system discussed for the previous system cannot be

made without the addition of an extra dimension due to the extra degree of freedom in the system. Correspondingly, any unique change in the magnesium solubility in iron rich phase and the iron solubility in the magnesium rich phase must now be a function of both the silicon concentration and the alloying element concentration in each of the liquid phases. Thus the immiscibility gap for the Fe-Si-Mg-X system can be established by suitable chemical analyses of the liquid phases.

2. Vapor Pressure Determination

Vapor pressure data can be reliably determined by many quite different techniques. Nesmeyanov,[16] in an extensive review of the subject, has shown the choice of experimental technique to be very dependent upon the temperature range of interest and the magnitude of the corresponding vapor pressures. For pure magnesium at 2650°F, an extrapolation of the available data yields a vapor pressure of 10 atmospheres[T]. Under these conditions, a variation on the basic liquid boiling method is recommended. The method is based on the observation that a liquid boils when the pressure of its saturated vapor is equal to the external pressure.

In 1929, Hartmann and Schneider[17] published vapor pressure data for magnesium obtained from a series of boiling experiments. These data have been considered to be quite accurate by various reviewers.[16,18,19] Their technique involved measurement of the temperature of a stagnant bath and the vapor temperature at a point just above the bath. With a decrease in the ambient pressure over the bath, boiling (or ebullition) could be made to occur. At that point, the temperature difference between the bath and the vapor decreased

to about 20°F from an initial condition of approximately 90°F difference. Also, the indicated vapor temperature profile remained constant over a small incremental distance above the bath surface and then decreased sharply. The reported experimental values were the indicated vapor temperature and the vessel pressure.

Nesmeyanov considers the boiling method to be one of the most reliable methods for the determination of high vapor pressures, providing that the experimental technique can accurately delineate the condition of boiling. Temperature and pressure can be reliably determined by various conventional techniques. However, these data become meaningful only when they are obtained under a defined condition of boiling. In the experiments of Hartman and Schneider, the state of boiling was determined by the decreased temperature difference between the bath and the vapor and also by the presence of the constant temperature zone immediately above the bath surface.

The experimental method used in the present investigation is derived from that of Hartman and Schneider. The idealized model will be considered at this point. As shown schematically in Figure 1a, the melt is contained in a crucible and is heated inductively. Since under these conditions, all the heat is generated within the melt, the net heat flux is outward from the melt to the colder vessel walls. The two thermocouples, as shown, measure the melt temperature and the vapor temperature, respectively. The inert gas pressure over the melt is variable as desired. For a typical experimental run, the power input is adjusted such that the bath temperature is constant at the temperature of interest. The vessel pressure, initially at some pressure

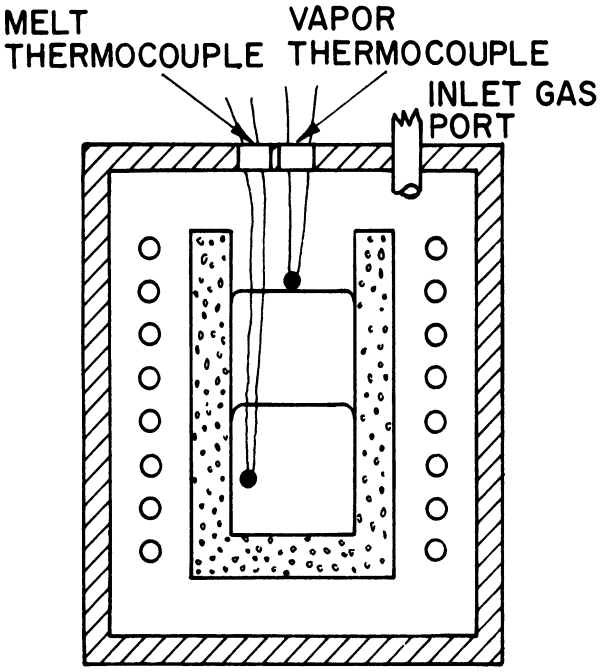

(a) Idealized Experimental Conditions.

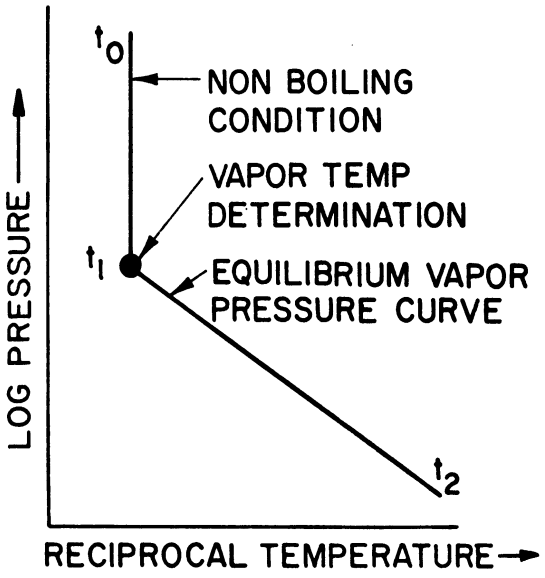

(c) Melt Temperature — Pressure Analysis. Data Transposed from (b).

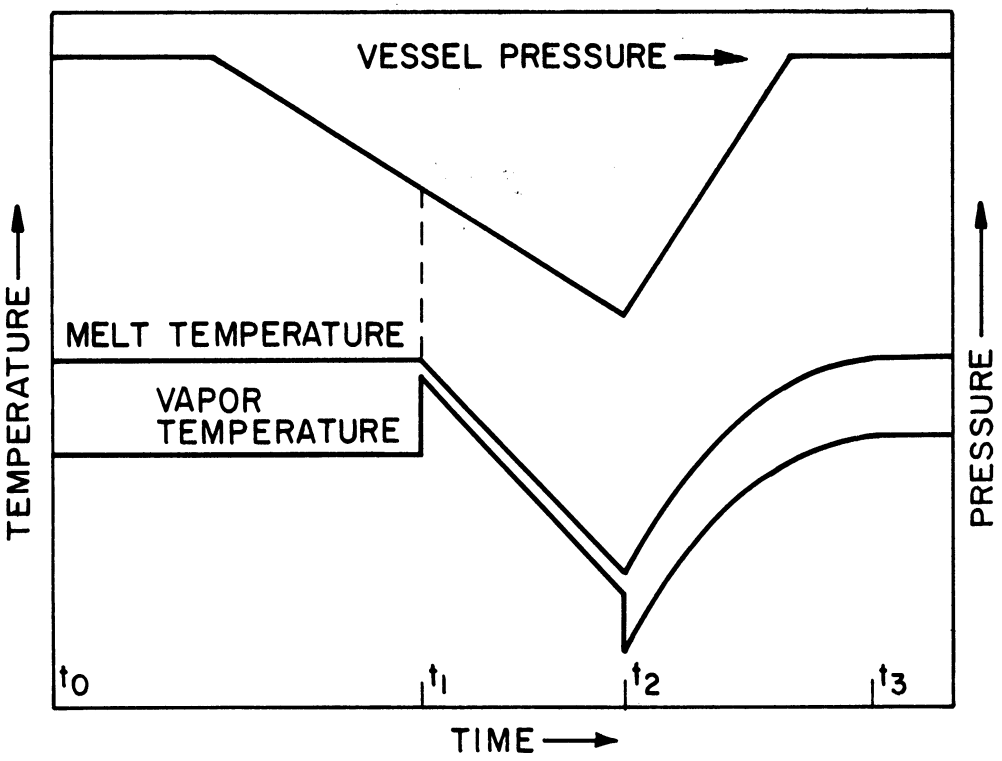

(b) Pressure and Temperature Profiles Over the Course of an Idealized Experiment.

Figure 1. Idealized model for vapor pressure determination under boiling conditions.

above that of the corresponding equilibrium vapor pressure, is then decreased by bleeding off some of the inert gas.

As shown in Figure 1b, the thermocouples will not indicate any temperature changes until the ambient pressure reaches the equilibrium vapor pressure. At that point, time t_1, boiling ensues and the melt temperature decreases, due to the heat required for vaporization. Simultaneously at time t_1, the vapor thermocouple indicates a higher temperature due to increased convective heating from the escaping vapors. The system is now in a state of equilibrium boiling; if the pressure is dropped still further, the temperature will drop correspondingly as more liquid is vaporized. However, when the inert gas pressure is increased to its initial value at time t_2, boiling ceases immediately and the melt temperature slowly increases to its initial value at time t_3. Simultaneously at time t_2, the vapor temperature decreases sharply due to the decreased convective heating.

There are two independent sets of vapor pressure relations which can be developed from the data of an experiment of this type. First, at the point where the vapor temperature thermocouple indicates a sharp temperature rise, a condition of boiling is indicated. Therefore, the pressure and melt temperature values at that point define a point on the vapor pressure-temperature curve.

The second set of vapor pressure relations is derived from a consideration of the melt temperature as a function of ambient pressure. If the melt temperature is plotted against the ambient pressure on a conventional logarithm pressure versus reciprocal temperature graph, as shown in Figure 1c, the state of boiling can be defined. Prior to the onset of boiling, only the pressure

is changing, while the temperature remains constant. The data thus plot as a vertical line. However, when boiling occurs, both pressure and temperature decrease. The plotted data then reflect the Clausius-Clapeyron vapor pressure relation,

$$\frac{d(\ell nP)}{d(1/T)} = - \frac{\Delta H_{vap}}{R} \quad ,$$

which is a straight sloping line on a log P versus 1/T coordinate system. Again, a condition of boiling can be defined and the meaningful pressure and temperature values can be delineated.

An experiment of this type thus satisfies the basic requirements of a boiling experiment in that temperature, pressure, and the condition of boiling are precisely defined. The two sets of vapor pressure data determinations can be compared to provide a check on the validity of the experimental technique. The data derived from the second method of analysis also define the vapor pressure as a function of temperature, which adds to the utility of the data.

B. EXPERIMENTAL EQUIPMENT

1. Pressure Vessel

The pressure vessel originally built by Trojan[9] and later modified by Sponseller[10] comprises the major piece of equipment used in this study. The basic vessel, shown in Figure 2, was originally designed to be experimentally versatile and therefore only slight modifications were necessary for this investigation.

Figure 2. The pressure vessel and auxiliary equipment used in the investigation.

The essential vessel components and their relative placement are shown in Figure 3. The rack and pinion mechanism was reconstructed to permit remote indexing of various devices over the melt. The four-station control head, located adjacent to the induction coil, can be moved vertically over a range of 4 inches and rotated through 360°. Vertical location is indicated on a calibrated dial to an accuracy of 0.05 inch. Rotational location is achieved to an accuracy within 2° by moving the lower rotating levers against a hinged stop.

Prior to the experimental work, the various pressure vessel components were disassembled, inspected, and reassembled. The pressure gauges were cali-

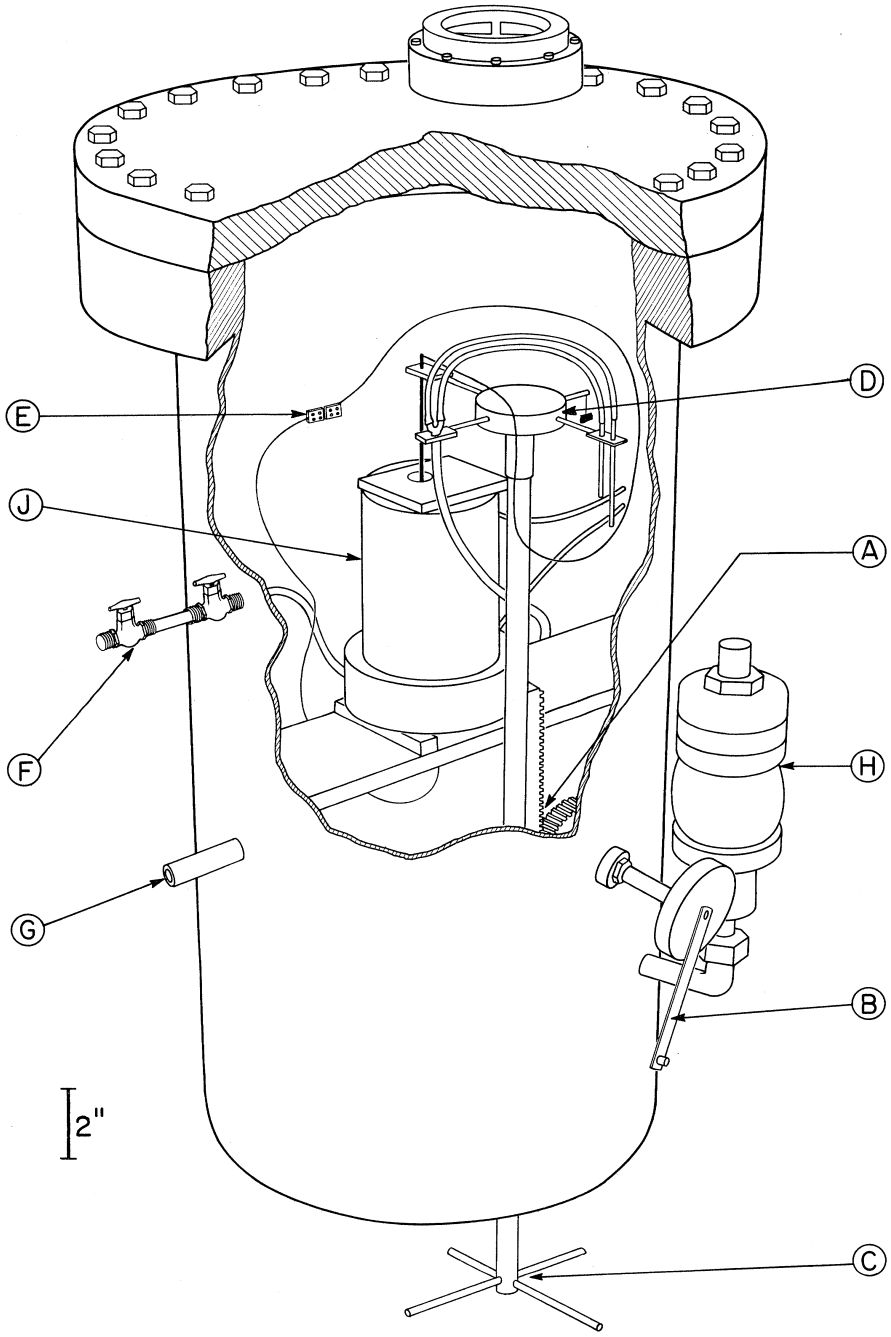

A. Elevating Rack and Pinion Mechanism

B. Elevating Lever

C. Rotating Levers

D. Four Station Control Head

E. Thermocouple Port

F. Sampling Needle Valves

G. Argon Port

H. Safety Relief Valve

J. Induction Coil Assembly

Figure 3 Sectional view of pressure vessel showing interior details.

brated using a hydraulic dead weight tester. The unit was then pressure tested to 750 psig. The new 600 psig emergency relief valve was also tested to insure the proper relief pressure and provide an index of the speed of the relief.

2. Crucible Preparation

The presence of both magnesium and iron along with third and fourth elements in solution at high temperatures posed a unique container problem. Refractory metals such as molybdenum, tantalum, and tungsten have been shown to be very resistant to attack by molten magnesium.[20] However, they can be readily dissolved in molten iron. Conversely, the results of Trojan[9] and Sponseller[10] indicated that commercial crucibles such as magnesia, alumina, zirconia, etc., would probably fail prematurely due to selective attack of the binder materials by the highly reactive magnesium. Chiotti, et al.,[21] experienced similar problems with graphite, beryllia, and magnesia crucibles in contact with liquid uranium and magnesium. However, they successfully used a crucible made from high purity magnesium oxide with 10 percent magnesium fluoride added as a binder. This formula was selected for this study since both the binder and the matrix are magnesium compounds; possible melt contamination from the crucible is thus minimized.

The crucibles used in the investigation are prepared by a tamping method with a magnesium fluoride content of 15 percent as recommended by Chiotti.[22] The reagent grade magnesium oxide and magnesium fluoride powders are mixed for 6 hours in a ball mill and then vacuum dried at 250°F for 12 hours. The temperature well is prepared by tamping the powder mixture into the die assembly

shown in Figure 4. This is done on a vibrating table in order to achieve the maximum possible density. After tamping, the inner metal form is removed and the graphite sleeve which contains the powder compact is placed in a graphite cylinder which will act as a susceptor in an induction field. This assembly is then placed in the induction sintering furnace shown in Figure 5. A sight tube is placed over the susceptor so that the temperature of the compact can be determined with an optical pyrometer. The susceptor and the lower portion of the sight tube are insulated by 100 mesh graphite powder which also minimizes oxidation of the susceptor. The assembly is heated to 2650°F in a period of about 20 minutes. The sintering reaction occurs over a temperature range of approximately 1900°F to 2200°F. This is determined from the gross shrinkage observed at these temperatures. After cooling to room temperature, the well is removed and ground slightly to remove surface imperfections.

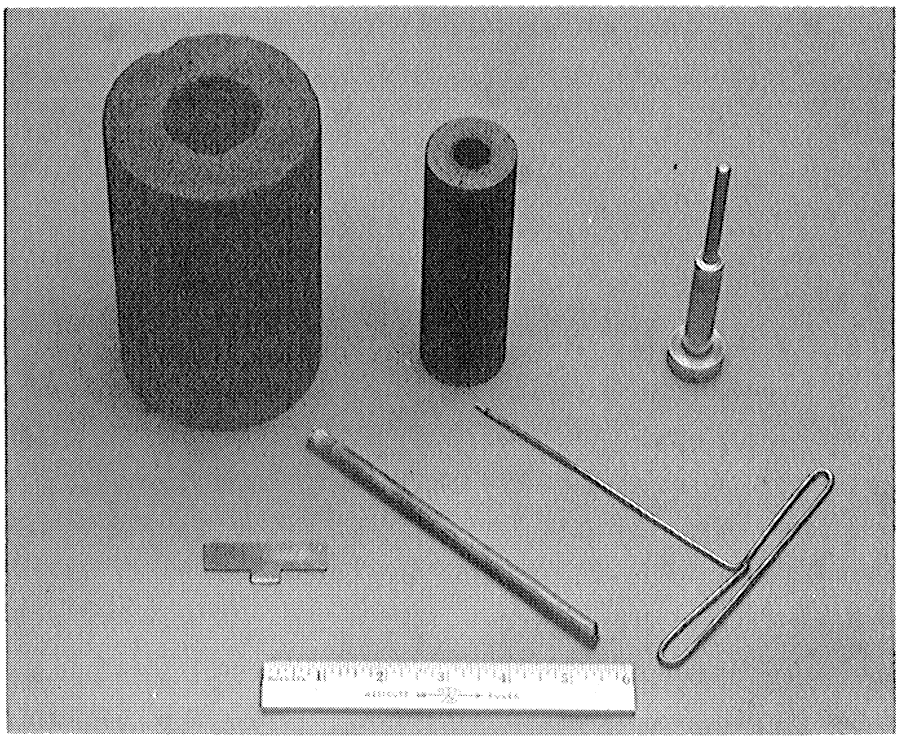

Figure 4. Temperature well die and fabricating tools.

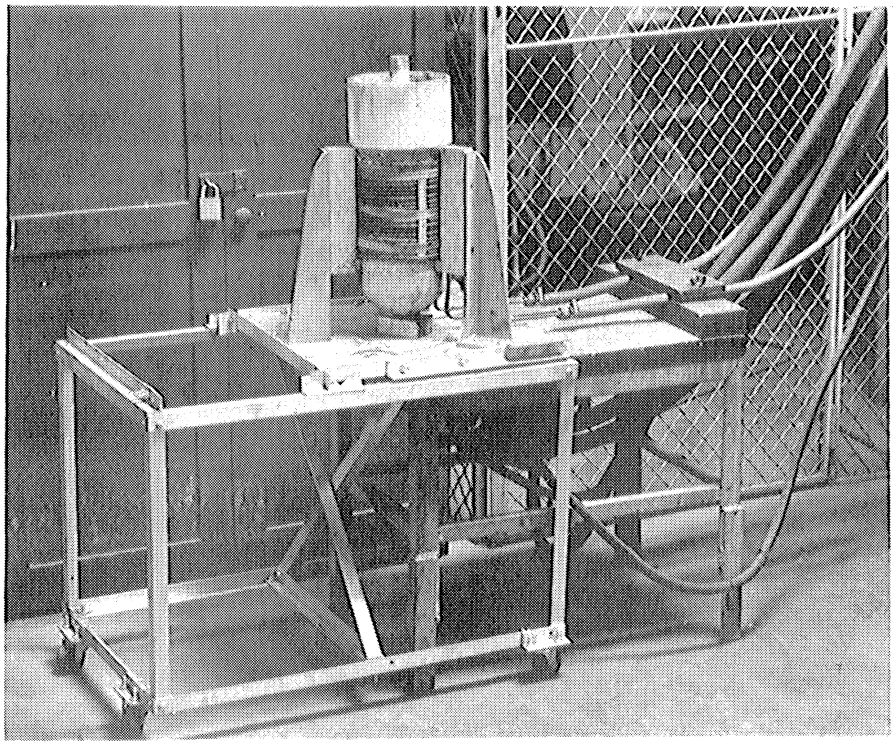

Figure 5. Induction sintering furnace used in crucible fabrication process.

The crucible is then tamped in the same manner as is the temperature well. The various materials used to make the crucibles are shown in Figure 6. After tamping, a hole is drilled in the center of the base into which the pre-sintered temperature well is inserted. The base is then covered with a graphite plug and the assembly is placed in the induction sintering furnace. The crucible is heated to 3000°F in about 90 minutes. After firing, the crucible is ground slightly to a uniform diameter and decarburized at 1750°F for 12 hours in a conventional muffle furnace. Figure 7 shows a powder compact, a sintered crucible, and a finished crucible ready for use.

The crucibles shrink about 40 percent during sintering and thus are prone to cracking if the powder is not uniformly packed or if the sintering heat is applied too rapidly. Therefore, all crucibles are leak tested with alcohol to verify the lack of cracks or continuous porosity.

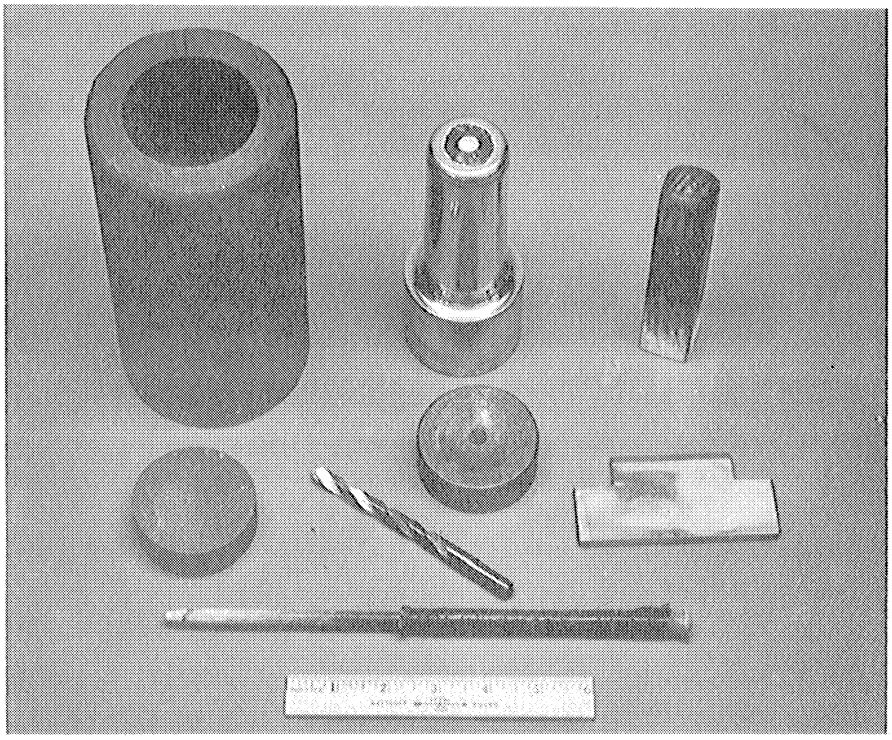

Figure 6. Crucible die components and fabricating tools.

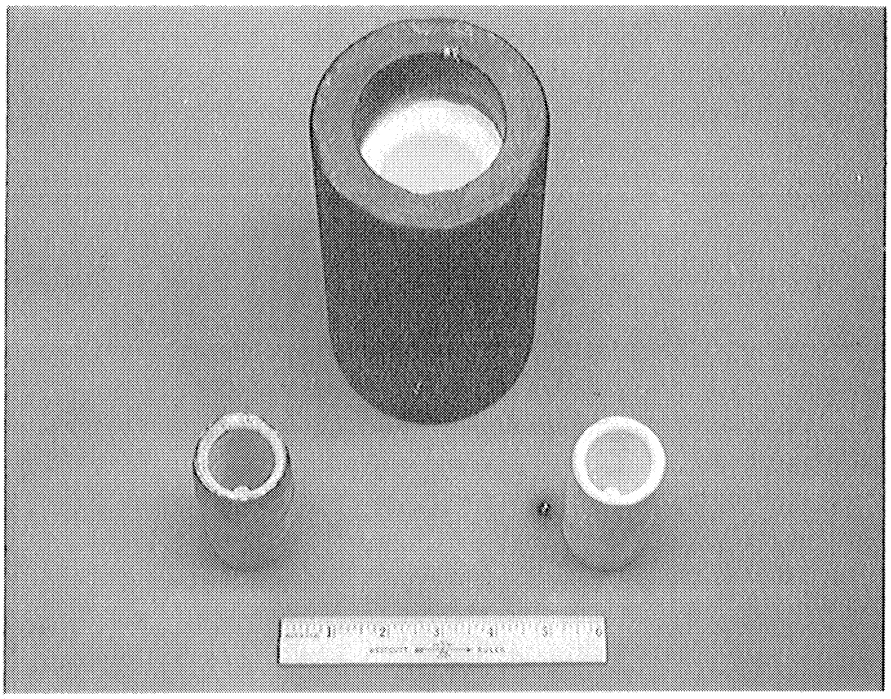

Figure 7. Powder compact, sintered crucible, and finished crucible.

Over the course of the investigation, certain disadvantages associated with these crucibles became apparent. The crucibles are prone to mechanical failure by either thermal shock or unrelieved expansion of a compacted metal charge. A disproportionate amount of time and labor is required to produce an acceptable crucible. Additionally, even though the melt thermocouple is encased in an alumina sheath, a few instances were noted of corrosive attack of the sheath and thermocouple by the crucible material. This attack is evidenced by premature thermocouple failure. Significantly, there has been no evidence of chemical attack of the crucible walls by the metal bath.

3. Temperature Measurement and Control

Melt temperatures are measured with a platinum-platinum 10 percent rhodium thermocouple located within the temperature well of the crucible. Initial trials indicated the thermocouple to be susceptible to attack by the fluoride ions in the crucible body, which lead to a premature catastrophic failure. This failure was remedied by enclosure of the thermocouple within an alumina sheath. The thermocouple assembly and placement are shown in Figure 8.

The thermocouple leads are connected through asbestos wrapped compensating leads to the main control panel. At this point, by means of switching circuits, the output can be directed either to one of two continuous temperature recorders or through a bucking circuit to the other recorder. The bucking circuit is incorporated so that a reference voltage from a small laboratory potentiometer can be added to the thermocouple output voltage, thus extending the range of the recorder. There is also provision for the switching

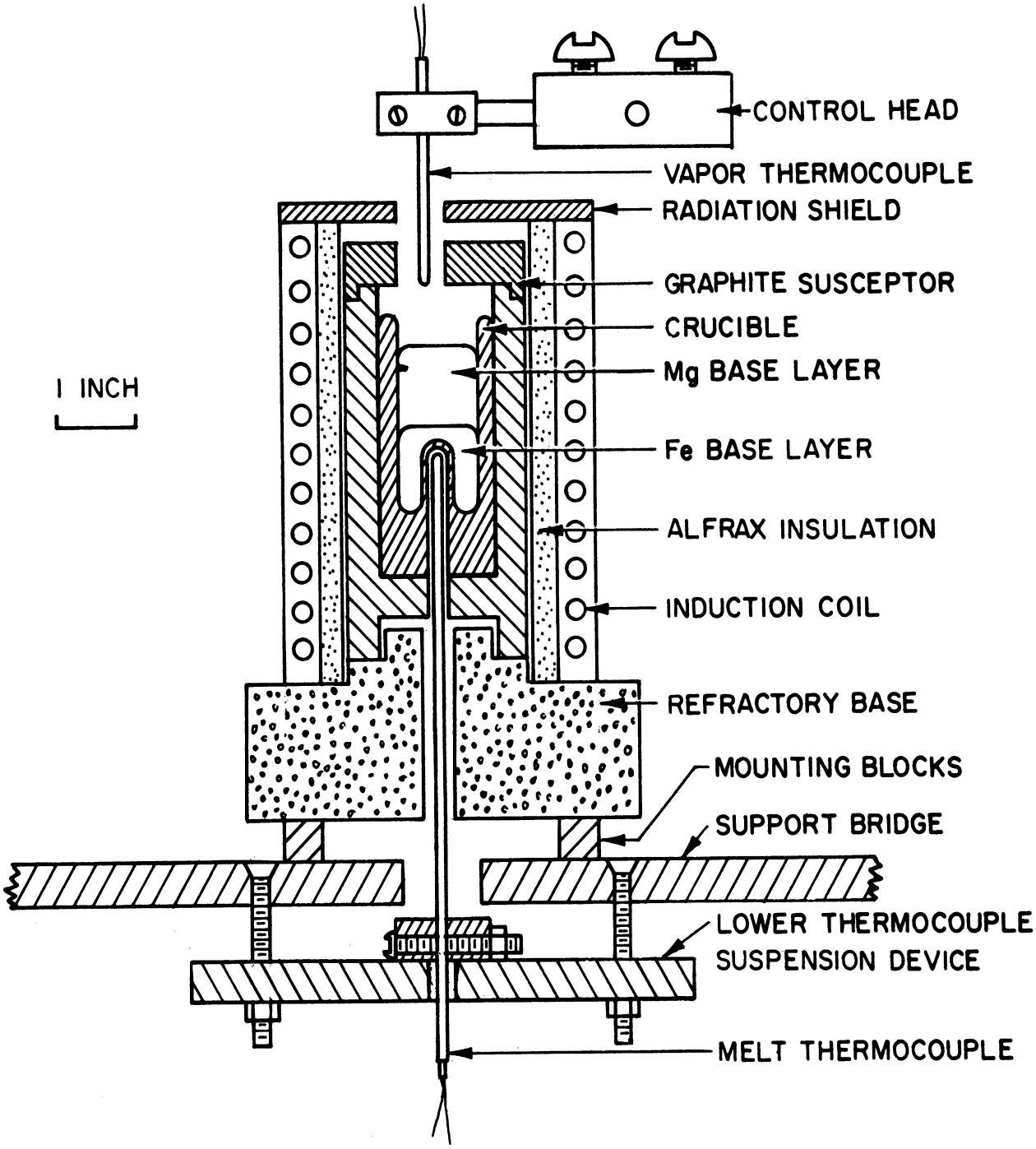

Figure 8. Thermocouple placements for melt and vapor temperature measurement.

of a semi-precision potentiometer into the circuit to permit calibration and standardization of the recorders.

The accuracy of temperature measurement was determined in two separate heats by comparing the temperature indicated by the melt thermocouple with

the temperature indicated by a second thermocouple protected by an alumina sheath suspended in the bath. For both heats, the indicated temperature difference was less than 10°F, measured with a precision potentiometer. After the second heat, the two thermocouples were checked against a platinum/platinum-10 percent rhodium secondary standard thermocouple which had been previously calibrated by the National Bureau of Standards. No significant drift in calibration was observed and thus it was presumed that there was no appreciable contamination of the respective thermocouples.

To insure consistent accuracy in temperature measurement, the thermocouple hot junctions are cut back 1/2 inch after each heat and rewelded. All of the thermocouple wire used in the investigation came from one calibrated lot. Additionally, one of the recorders was factory calibrated at the outset of the investigation.

The melt temperature is controlled by manual adjustment of the input power. Since there is no electrical feedback from the melt thermocouple, a certain amount of overshoot can occur. However, the indicated temperature could be maintained within 10°F of the desired temperature after an adjustment period of 2 minutes. Considering all the possible sources of error, it is estimated that the indicated temperature lies within 10°F of the true temperature. Therefore, the true temperature is estimated to be within 20°F of the desired temperature for any particular heat.

4. Boiling Determination for Vapor Pressure Measurement

In the previous section dealing with the design of the vapor pressure experiments, three simultaneous and continuous measurements were shown to be re-

quired. These are the bath temperature, the vapor temperature, and the ambient vessel pressure. The bath temperature is monitored continuously by one of the recorders as described previously. The vapor temperature is monitored on the second recorder by means of a thermocouple suspended from the main control head, as shown in Figure 3. At the time of the vapor pressure experiment, the vapor thermocouple, enclosed in an alumina sheath, is positioned just below the susceptor cover, as shown in Figure 8. At this position, the indicated vapor temperature is 300°F to 400°F lower than the bath temperature. Attempts to determine the vapor temperature immediately above the bath surface were largely unsuccessful as the relative position of the surface changes appreciably with small changes in the inductive power input.

The ambient vessel pressure is monitored at discrete incremental values. As the vessel pressure is decreased over the course of an experiment, pressure values are read from the gauges on the control panel. At 10 psig intervals, a null button is manually pressed. This action produces a direct short across both thermocouple outputs with the observable effect being an inflection on both strip chart records. The estimated accuracy of pressure measurement is ±1 psig.

The temperature records from a typical vapor pressure experiment are shown in Figure 9, transposed to one figure for clarity in presentation. The melt temperature profile decreases toward the end of the experiment, implying a condition of boiling. Concurrently the vapor temperature profile increases to a sustained peak. As the pressure is subsequently increased, the respective temperatures revert to their original values. The analysis of such a

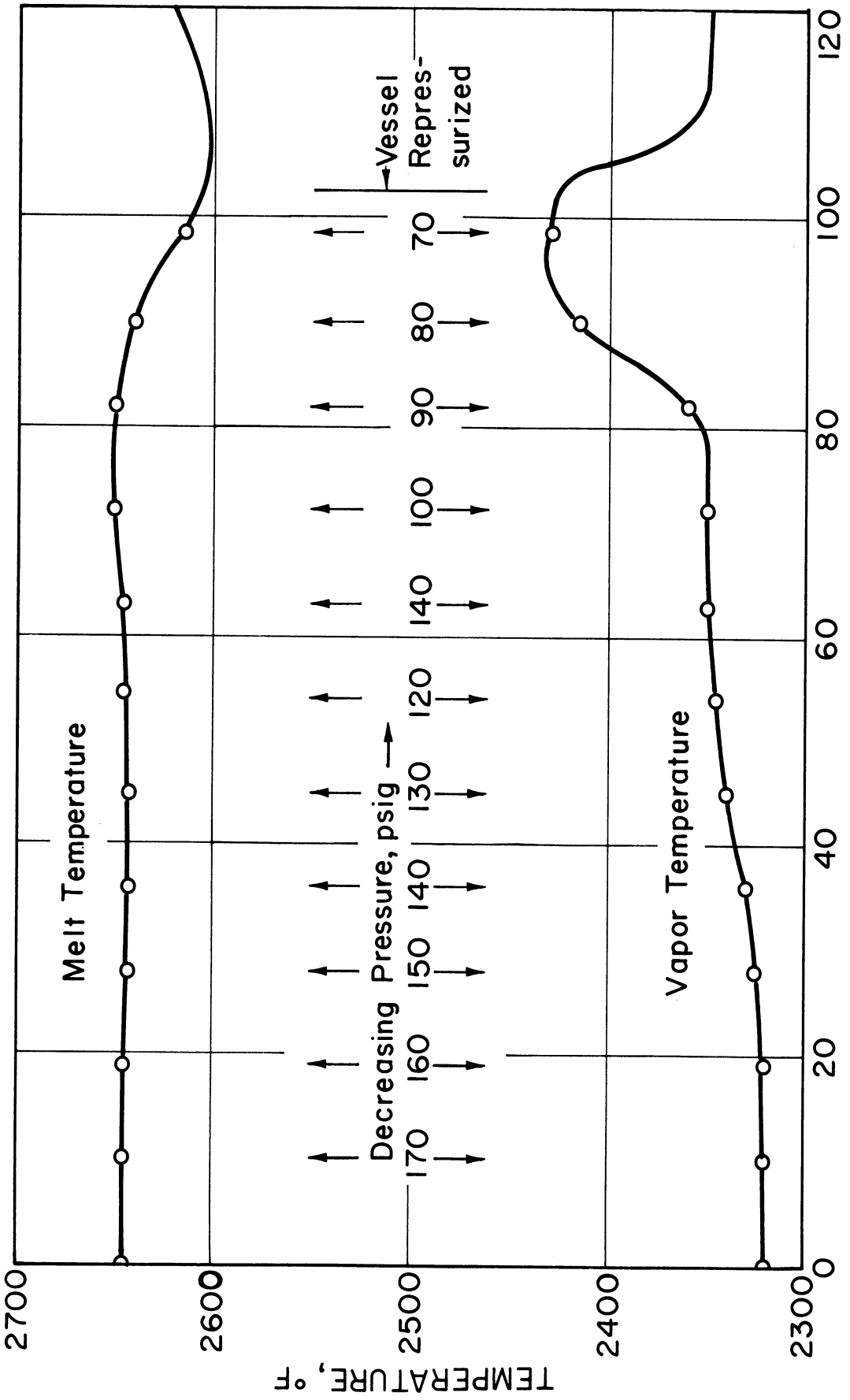

Figure 9. Temperature-pressure relationships during a typical boiling experiment (Heat 238).

record will be presented later in the report.

5. Bath Sampling Device

The sampling operation requires inserting two tubes of different length into the bath so that one enters each liquid layer. A representative sample is drawn into each of the tubes; the tubes are then immediately removed from the melt.

Extreme care must be taken to insure that representative and sufficient samples are removed for subsequent chemical analysis. The magnesium-base liquid is superheated approximately 1500°F above its liquidus temperature. The results of Trojan[9] show that considerable segregation can occur if the samples are not rapidly frozen. Conversely, the iron-base liquid is superheated only about 200°F to 300°F above its liquidus temperature, thus presenting a fluidity problem. If this liquid sample is frozen prematurely, an insufficient sample will be obtained. The sampling operation is further compounded by the extreme difference in densities of the two-liquids. Thus, for a given pressure differential, the magnesium-base sample will rise higher into a sampling tube than will the iron-base sample.

After experimental evaluation of several designs, the sampling device described in Figure 10 was developed. The iron-base liquid sampling tube is an alumina tube cemented inside a molybdenum tube to protect against thermal shock. The magnesium-base liquid sampling tube consists of a molybdenum tube with constricting alumina orifices cemented in at the bottom and top. During the sampling operation, the bottom orifice impedes the flow of the magnesium-base liquid into the sampler. The upper orifice acts both to reduce the pres-

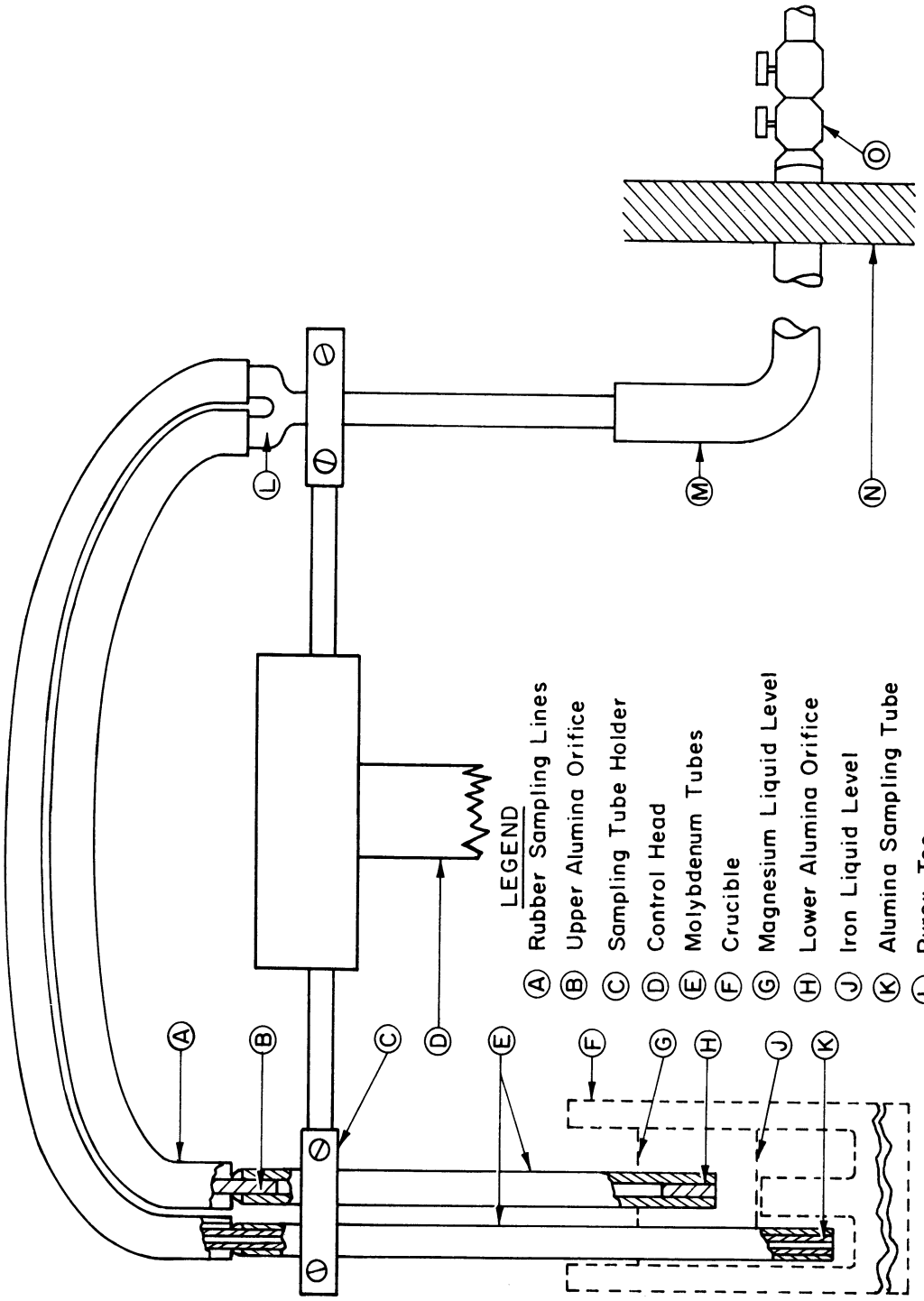

Figure 10. Sampling device and sampling lines.

sure differential used to draw the sample up and also prevents further flow once the tube is filled. This combination of a flow restricting sampler for the magnesium-base liquid and an open sampler for the iron-base liquid yields sufficient and representative samples for chemical analysis.

The pressure differential necessary to force the respective liquids into the samplers is developed by bleeding argon from the sampling line to the atmosphere. This is done after the samplers are positioned within the melt. Argon gas flow control is maintained by suitable adjustment of the needle valves located on the outside of the vessel.

6. Raw Materials

The possible influence that small amounts of impurity elements can have on solubility relationships makes the choice of raw materials important. The materials listed in Table I were used for this investigation.

C. CONDUCT OF A TYPICAL EXPERIMENT

1. Component Assembly

After the various sub-components described in previous sections have been fabricated, a trial assembly is made outside the pressure vessel. The melt thermocouple is adjusted on the thermocouple bridge so that it extends to within 1/32 inch of the top of the crucible temperature well, as shown in Figure 8.

The components are then reassembled within the vessel. The melt thermocouple circuit is checked by placing a heated refractory tube around the exposed thermocouple and observing the recorder response. Next, the crucible is inserted and the sampling device is attached to the control head. The relative

TABLE I

CHEMICAL ANALYSIS OF RAW MATERIALS

Material	Supplier	Major Impurities
Ferrovac 'E' vacuum-melted iron	Crucible Steel Company	Ni 0.035 pct Si less than 0.03 pct Cu 0.01 pct Cr less than 0.01 pct S 0.005 pct C 0.004 pct Al less than 0.003 pct P 0.002 pct Mn 0.001 pct Mg less than 0.001 pct Ca less than 0.001 pct
Primary stick magnesium	Dow Metal Products Company	Al less than 0.03 pct Ca less than 0.01 pct Cr less than 0.001 pct Fe 0.036 pct Mn less than 0.03 pct Ni less than 0.001 pct Pb less than 0.01 pct Si less than 0.01 pct Sn less than 0.01 pct Zn less than 0.02 pct Be less than 0.0001 pct
Electronic grade silicon	Texas Instruments, Inc.	Less than 0.0001 pct total impurities
Zirconium	Mallory Sharon Metals Company	Fe 0.031 pct C 0.025 pct Si 0.006 pct Mn 0.002 pct O 0.116 pct
Electrolytic manganese	Union Carbide Company	Less than 0.1 pct total impurities
Cobalt strip	Sherritt Gordon Mines, Ltd.	Ni 0.10 pct Cu 0.005 pct Fe 0.018 pct C 0.014 pct S 0.004 pct
Graphite 'G' carbon	Graphite Specialties, Inc.	Less than 0.5 pct total impurities

positions of the separate sampling tubes are adjusted so that when the control head is at its lowest position, the iron-liquid sampling tube extends to within 3/16 inch of the crucible bottom and the magnesium-liquid sampling tube is located about 3/8 inch above the temperature well. After the sampling lines are attached, the samplers are rotated to the side and the crucible is removed for volume measurement.

The crucible volume is measured by adding alcohol from a burette. Two volumes are measured, the volume of alcohol required to just cover the temperature well and the total volume up to a level 5/8 inch from the top of the crucible. These volumes, which represent the desired volumes of the iron-rich liquid and the total melt, respectively, are used to calculate the charge composition. The computation is based upon the elemental liquid densities, the measured volumes, and an assumed silicon partition. Although it is not precise, the results represent an adequate estimate.

After the crucible is replaced in the vessel, the charge is added. A typical charge, weighed to within 0.1 gram, is placed in the crucible in the following sequence. The crushed silicon chips are placed in the bottom up to the top of the temperature well. Then the magnesium slug, cut from a cylindrical rod, is placed in the crucible. The iron slug is placed on the magnesium and any remaining silicon chips are poured into the space between the slugs and the crucible wall. For those heats in which a fourth element is added, the required amount is placed at the bottom with the silicon chips.

After the crucible cover and the radiation shield have been positioned, the susceptor plug is attached to the control head. This plug, which fits

loosely within the access hole, prevents undue vaporization losses and heat losses. The vapor thermocouple is then attached to the control head and tested for proper response. Lastly, the vessel cover is lowered into position and bolted down.

2. Heat Procedures

Before turning the power on, the vessel is evacuated to 500 microns pressure for 1 hour, flushed with argon gas and then evacuated again for 1/2 hour. The charge is heated at a rate of about 200°F per minute to about 2000°F and then at a rate not exceeding 100°F per minute. Argon gas is added when the temperature reaches 600°F to a pressure of 25 psig. Additional argon gas is added in several stages, paralleling the temperature rise, until the working pressure is achieved. As the temperature approaches the desired experimental temperature, the power input is adjusted so that this temperature is maintained.

The major portion of the solubility study has been conducted at a working temperature of 2650°F. This temperature exceeds the liquidus temperatures across the magnesium-silicon phase diagram and similarly exceeds the liquidus temperatures across the iron-silicon phase diagram for silicon contents greater than 5 percent.[5] Several heats were also conducted at 2550°F and 2750°F to establish the temperature sensitivity of the immiscibility relations. Since the extrapolated vapor pressure of pure magnesium ranges from 95 psig at 2550°F to 182 psig at 2750°F, the minimum working pressures necessary to prevent boiling are established approximately 60 psi higher than the extrapolated vapor pressure, i.e., from 150 psig to 250 psig.

After holding at temperature for 2 minutes while making the final minor power adjustments, the susceptor plug is lifted and the vapor thermocouple is moved into position. The switching circuit is set so that the melt temperature is indicated on one recorder while the vapor temperature is indicated on the second recorder. When the vapor thermocouple is indicating a steady value, the exhaust valve is opened slightly. As the vessel pressure decreases, the null button is pressed at 10 psi intervals. After the vapor thermocouple has indicated a sharp temperature increase and the melt temperature has dropped 30°F to 50°F, the exhaust valve is closed. The vessel is then repressurized to the initial pressure setting. The vapor thermocouple is lifted and the sampling device is rotated into position. A short delay occurs while the bath temperature increases to the initial temperature. The power is then turned off and the samplers are plunged into the melt. After a delay of 3 seconds, to allow the samplers to be heated slightly, the sampling valve is opened and samples are drawn up into the respective samplers. The sampling device is then lifted and the susceptor plug is moved back into its initial position.

This entire procedure requires 5 to 6 minutes to complete, measured from the time at which the working temperature initially is reached until the samples are taken.

3. Time to Attain Equilibrium

An important experimental factor is the time at temperature to establish dynamic equilibrium between the phases. This variable was investigated by making a special series of heats within a narrow bulk composition range at

2650°F. Samples were taken after the melt had been at temperature for 10 seconds, 2, 5, 6.5, and 15 minutes. The resultant chemical analyses are listed in Table II. The general trend of the data, Figure 11, shows that

TABLE II

CHEMICAL ANALYSIS OF TIME-TO-EQUILIBRIUM HEATS

Heat No.	Holding Time	Iron-Base Liquid %Mg	Iron-Base Liquid %Si	Magnesium-Base Liquid %Si	Magnesium-Base Liquid %Fe
181	10 sec	2.21	17.13	6.10	2.66
210	10 sec	2.45	16.58	4.94	2.44
257	10 sec	1.78	16.81	*	
83	2 min	1.94	17.49	7.01	3.30
282	2 min	2.01	16.99	*	
135	5 min	1.94	16.27	4.38	2.81
143-1***	5 min	2.18	16.91	* *	3.96
-2		2.20	17.21	* *	3.47
209	5 min	* *	16.03	4.65	2.13
146-1***	6.5 min	2.17	16.83	* *	2.52
-2		2.18	16.99	* *	2.93
183	15 min	2.32	17.19	5.71	1.69
227	15 min	2.56	17.74	*	

*Sample not obtained.
**Analysis not obtained.
***Duplicate samples from same melt.

equilibrium is attained within a time period of less than 5 minutes. Those points showing the greatest deviation from the general grouping are from heats equilibrated for 10 seconds and 2 minutes. The scatter of these data around the overall ternary solubility curve (discussed later in the results section), implies that the variance in chemical analysis (particularly in the magnesium-rich samples) and the interdependence of magnesium solubility and silicon content are at least as significant as the equilibration time.

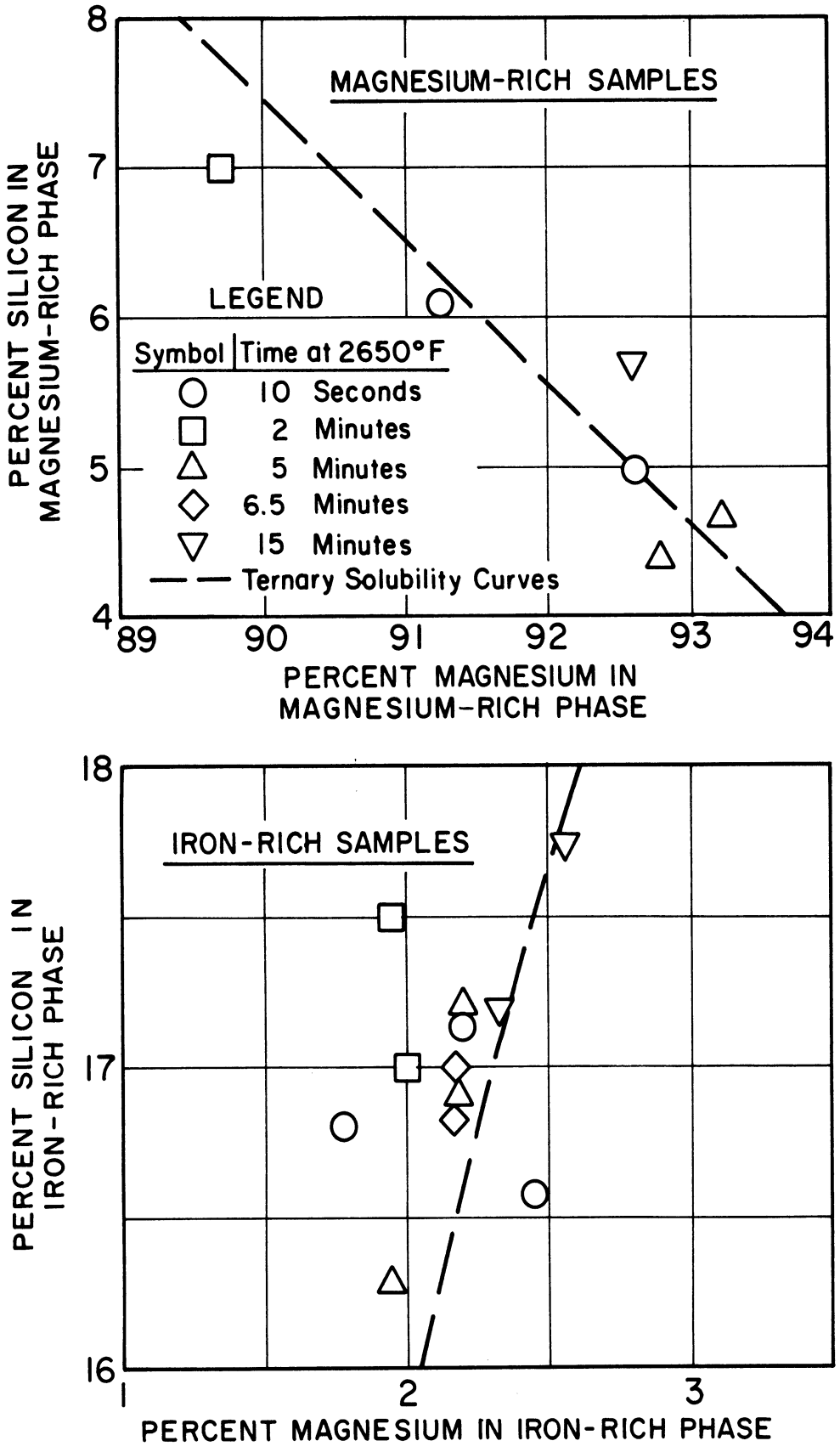

Figure 11. Time at temperature to attain equilibrium in the iron-base and magnesium-base liquids.

This relatively rapid rate of equilibration is consistent with the results of Trojan[9] and Sponseller[10] which were 5 minutes and 3 minutes, respectively, for similar investigations.

D. INTERPRETATION OF EXPERIMENTAL DATA

A typical heat, as described in the previous section, yields the two samples from the equilibrated liquids and the two temperature records from the respective temperature recorders. The analysis techniques used to convert the samples and the temperature records to functional data are described in the following categories.

1. Chemical analysis techniques.
2. Magnesium vapor pressure analysis.
3. Regression analysis of data groups.

1. Chemical Analysis Techniques

The samples are analyzed in the analytical laboratory of an industrial research group. These determinations are not commercially routine and the techniques are quite specialized; however, the staff of the research laboratory routinely analyzes various special magnesium-ferrosilicon alloys and therefore is intimately familiar with the general procedures.

The specific analytical procedures are described in Appendix I.

The degree of segregation within a drawn sample was checked by analyzing two iron-base samples and one magnesium-base sample, each of which was cut into three portions. As shown in Table III, the magnesium content in an

TABLE III

SAMPLE SEGREGATION AND CHEMICAL ANALYSIS REPRODUCIBILITY

Heat No.	Sample No.	Iron-Base Sample %Mg	Iron-Base Sample %Si	Magnesium-Base Sample %Si	Magnesium-Base Sample %Fe
119	Top 1/3	2.98		*	*
	Middle 1/3	5.58	16.57	*	*
	Bottom 1/3		16.45	*	*
120	Top 1/3		17.25	5.92	22.10
	Middle 1/3	4.60	16.76	0.58	8.32
	Bottom 1/3	1.50		4.72	10.66
143	Sample 1	2.18	16.91	**	3.96
	Sample 2	2.20	17.21	**	3.47
146	Sample 1	2.18	16.99	**	2.52
	Sample 2	2.17	16.83	**	2.93
100	Sample 1	13.67	32.57	***	
	Sample 2	14.37	33.44		

*Sample not obtained.
**Analysis not obtained.
***Sampler mispositioning resulted in two iron-base samples.

iron-base sample can vary by a factor of three between different portions of the sample while the silicon content changes very little. Correspondingly, the iron and silicon contents are typically quite low in the middle portion of a magnesium-base sample compared to either end. These variances reflect rapid solidification at the top of a sample and settling of the heavier micro-constituents from the middle portion to the bottom as solidification progresses.

Chemical analysis reproducibility is also shown in Table III. For these heats, the experimental variance was minimized by simultaneously drawing two samples from the melt. As shown, the accuracy of magnesium analysis in iron is approximately ±0.5 percent of the amount analyzed at the 2 percent magne-

sium level (±0.01%Mg) and ±3 percent at the 14 percent magnesium level (±0.35 %Mg). Silicon in iron can apparently be determined to within ±0.9 percent of the amount analyzed at 17 percent Si (±0.15%Si) and to within ±1.5 percent at the 33 percent silicon level (±0.43%Si). A larger deviation would be expected for analyses of the magnesium base sample due to the more severe segregation possible; however, the solubility data do not indicate a severe scatter of points.

Trojan[9] indicated chemical analysis accuracy to be approximately ±2 percent of the amount analyzed for magnesium in iron at 1 percent levels. The analyses of the present investigation show a similar accuracy at considerably higher magnesium levels which indicates an equivalent if not higher degree of precision.

2. Magnesium Vapor Pressure Analysis

Two temperature records with accompanying pressure measurements are available from each heat. The vapor temperature record characteristically shows three distinct zones, as shown in Figure 9. Throughout the first zone, the vapor temperature remains fairly constant, showing only slight perturbations. The second stage is evidenced by an abrupt temperature rise of 100°F to 200°F. This temperature rise is sustained until the vessel is repressurized, at which time the vapor temperature drops to approximately its initial value. This region is denoted zone three. Likewise, the melt temperature, Figure 9, characteristically remains constant during the initial part of the experiment. Then, shortly after the vapor temperature shows an abrupt

temperature rise, the melt temperature decreases. This decrease is similarly sustained until the vessel is repressurized, at which time the melt temperature increases to its initial value. Vapor pressure data are derived from a consideration of both the nature of these two temperature profiles and the pressure and melt temperature values.

The initial, relatively constant temperature indicated by the vapor thermocouple reflects radiation from the bath, crucible, and susceptor, plus conduction up the sheath to the brass support arm, Figure 8. When boiling begins, the thermocouple is additionally heated by the effusing magnesium vapor giving rise to an abrupt increase in temperature. Next, as the vessel is repressurized, boiling stops and the vapor temperature decreases. Thus, at the point of the abrupt vapor temperature increase which indicates the initiation of boiling, a pressure value can be determined from the pressure reading at this point on the vapor temperature record. The corresponding melt temperature can be determined from the melt temperature record. In this way, each heat therefore gives a definite value of the vapor pressure of the melt at a chosen temperature.

The melt temperature record can be used to provide additional vapor pressure information. The initial portion of this temperature profile is maintained as level as possible by adjusting the power input such that all thermal losses are balanced. Then, during the experiment, when the pressure is lowered to initiate boiling, the heat required to vaporize the effusing magnesium results in a steady decrease of the melt temperature. Thus, the condition of boiling can again be defined, although not as distinctly as is possible when

considering the vapor temperature record.

However, if the set of vessel pressure-melt temperature values from the chart record are plotted as logarithm pressure versus reciprocal temperature, the curve indicated by these plotted points should approach the relations shown for the idealized case in Figure 1. Nonboiling conditions are shown by a vertical line and a negatively sloped line reflects the Clausius-Clapeyron relation between temperature and pressure under boiling conditions. Therefore, if these two line segments can be uniquely identified from the data, a condition of boiling can be defined and a relationship can be derived between vapor pressure and temperature.

The data interpretation can be best presented by consideration of an example. The heat data shown in Figure 9 are replotted in Figure 12 in the previously described manner. The melt temperature data indicate a slightly lower vapor pressure value (85 psig) than the vapor temperature data (90 psig). This is attributed to the slight thermal lag imposed on the melt thermocouple by the necessary shielding materials. However, the absolute difference, in general, is less than 5 psig regardless of the vapor pressure level measured.

As a means of estimating the relative accuracy of the method of determining vapor pressures, data were obtained for pure magnesium over a temperature range of 2300°F to 2800°F. These data, analyzed as described, are shown in Figure 13 and listed in Appendix II. A regression analysis of all the experimental data yields the relation

$$\text{Log Press. (atm)} = 4.928 - 1.220 \times 10^4/\text{Temp (°R)}, \pm 0.017 .$$

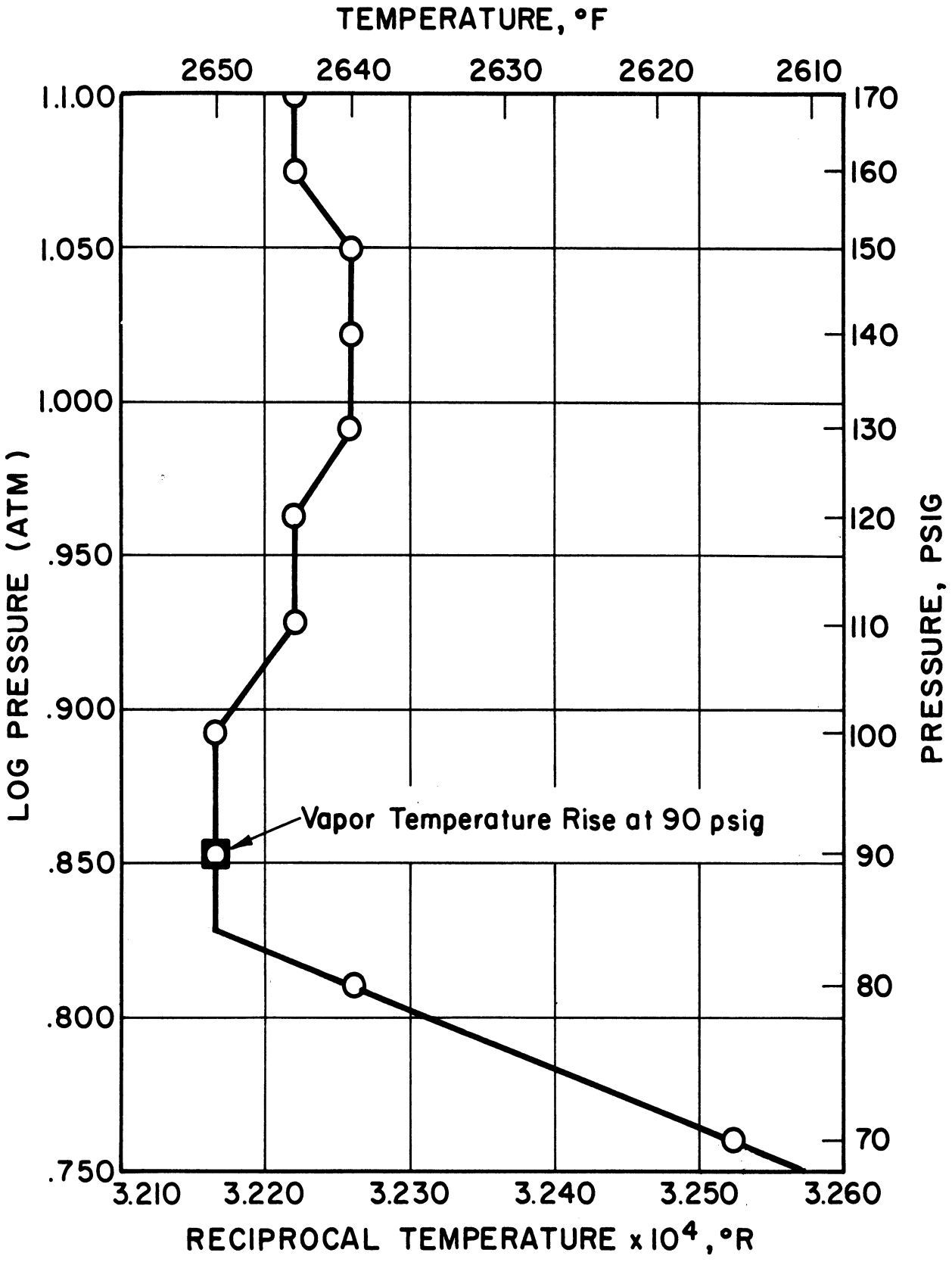

Figure 12. Data from Figure 9, Heat 238, replotted to show method of magnesium vapor pressure determination.

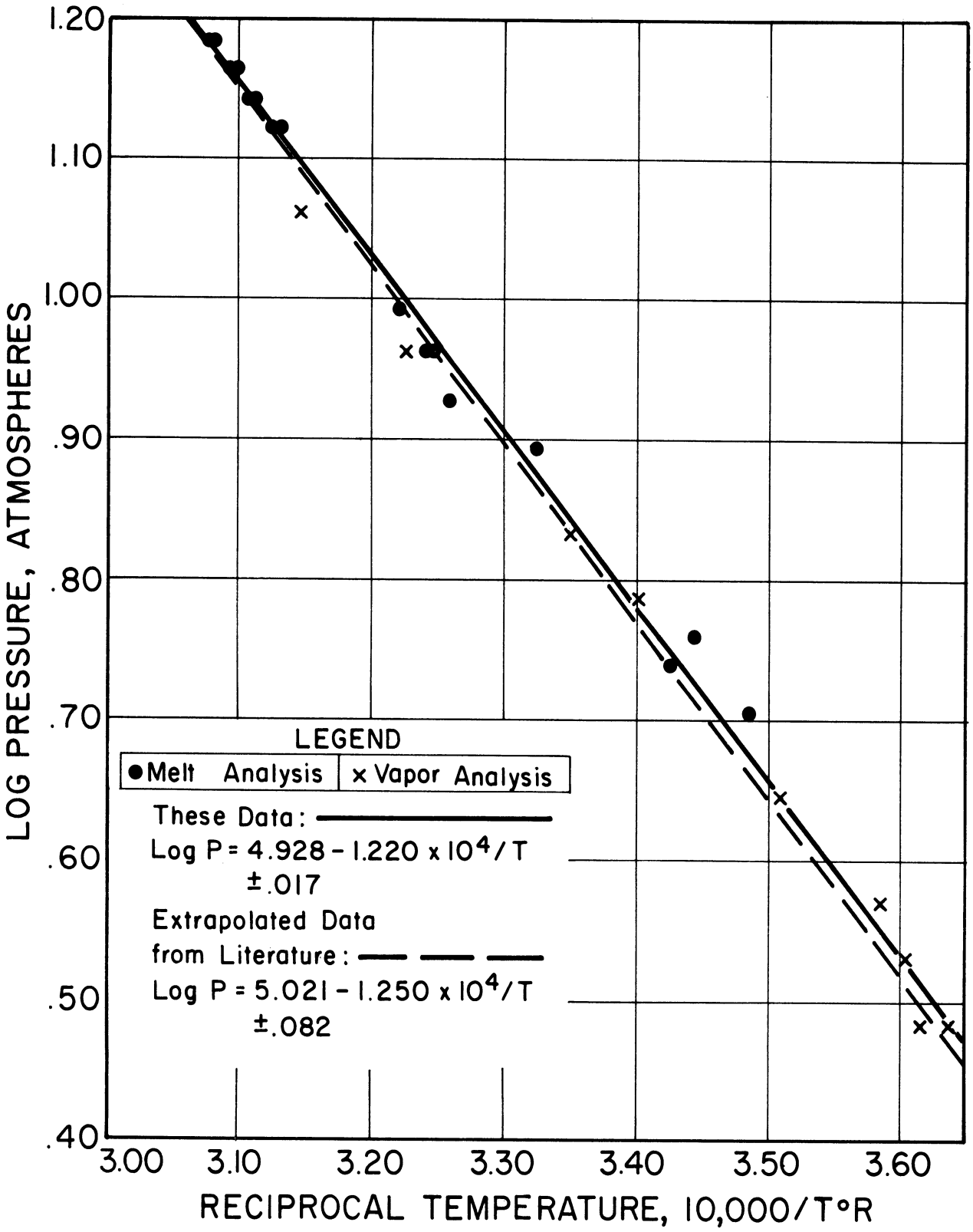

Figure 13. Vapor pressure of pure magnesium.

Since magnesium vapor pressure data for this pressure range were not available in the literature, the data of this study are compared with extrapolated low temperature data. Included are the results of those investigators[17,23,24,25] considered most reliable by Nesmeyanov[16] and Hultgren, et al.[18] A regression analysis yields the relation:

$$\text{Log Press. (atm)} = 5.021 - 1.250 \times 10^4/\text{Temp}(^\circ\text{R}) \pm 0.082 ,$$

as shown in Figure 13.

The vapor pressure of pure magnesium at 2650°F as predicted by the various analyses illustrates the validity and accuracy of the experimental technique. The absolute pressure values are:

Source	Predicted Vapor Pressure	Uncertainty
Extrapolated Literature Data	147.1 psia	± 28.3 psia
Experimental Vapor Temperature Data	141.9 psia	± 3.0 psia
Experimental Melt Temperature Data	151.0 psia	± 5.5 psia
All Experimental Data	148.6 psia	± 5.6 psia

As indicated by these values, the data of the present study are within the uncertainty of the extrapolated data and the combined data (vapor and melt temperature data) agree almost exactly with the extrapolated values.

3. Regression Analysis of Data Groups

The various solubility and vapor pressure data groups were analyzed using a standard regression method on a digital computer. The vapor pressure data

were fit to a linear equation. As shown in Appendix II, the format was designed so that pressure and temperature values are used for input and output data directly. For the solubility data, regression equations were calculated up to a fifth-order polynomial. The choice of best representation of the particular solubility data group is made on the basis of the calculated standard deviation and the characteristics of the plotted polynomial curve. The program format was also designed to allow average solubility data to be calculated, as shown in Appendix III.

IV. DISCUSSION OF RESULTS

The solubility and vapor pressure data obtained in the investigation are presented in Tables IV and V. These data and their significance will be discussed in the following sequence:

A. Experimental data.

B. Theoretical considerations.

C. Commercial applications.

A. EXPERIMENTAL DATA

For the sake of simplicity in discussion, the experimental data have been divided into several broad categories as shown below:

1. Liquid miscibility relations at 2650°F.

2. Temperature effects on magnesium solubility.

3. Magnesium vapor pressure over the miscibility gap.

4. Effect of fourth elements on magnesium solubility and vapor pressure.

1. Liquid Miscibility Relations at 2650°F

The liquid immiscibility data for the iron-magnesium-silicon ternary system, shown in Figure 14, form the basis for the discussion of the other equilibrium data. The liquid-solid equilibria in the iron-rich corner of the diagram were constructed from the data given by Hansen[5] for the binary iron-silicon system. The regression program shown in Appendix III was used to construct the profile of the miscibility gap. These regression calculations show an overall standard deviation of 0.48 percent magnesium for a fourth-order

TABLE IV

CHEMICAL ANALYSIS OF EXPERIMENTAL HEATS

Heat No.	Iron-Base Liquid			Magnesium-Base Liquid		
	%Mg	%Si	%X	%Si	%Fe	%X
			Basic Ternary Data at 2650°F			
68	*	*		29.58	17.01	
82	0.97	6.71		0.54	2.76	
100-1	13.67	32.53		***	***	
100-2	14 37	33.44		***	***	
135	1.94	16.27		4.38	2.81	
143-1	2.18	16.91		**	3.96	
143-2	2.20	17.21		**	3.47	
146-1	2.18	16.99		**	2.93	
146-2	2.17	16.83		**	2.52	
180	10.42	30.06		*	*	
181	2.21	17.13		6.10	2.66	
183	2.32	17.19		5.71	1.69	
207	*	*		4.11	2.77	
208	5.66	24.90		***	***	
209	**	16.03		4.65	2.13	
223	1.73	11.76		1.56	2.64	
225	6.17	23.43		*	*	
226	12.33	31.15		*	*	
227	2.56	17.74		*	*	
238	6.38	25.42		*	*	
242	0.90	5.84		*	*	
258	6.10	25.19		***	***	
259	10.75	30.92		*	*	
263	7.86	27.33		*	*	
264	11.57	30.00		*	*	
265	4.90	20.87		***	***	
278	10.43	29.56		30.38	17.94	
279	5.64	24.57		20.47	8.26	
280	3.87	21.18		14.43	4.47	
282	2.01	16.99		*	*	
			Ternary Data at 2550°F			
239	1.47	11.62		2.31	1.97	
261	8.11	29.36		23.74	9.35	

*Representative sample not obtained.

**Chemical analysis not obtained.

***Sampler mispositioning resulted in two iron-base samples.

TABLE IV (Concluded)

Heat No.	Iron-Base Liquid %Mg	%Si	%X	Magnesium-Base Liquid %Si	%Fe	%X
		Ternary Data at 2750°F				
240	2.58	11.67		2.40	2.79	
260	6.86	26.08		22.29	12.57	
		Quaternary Data at 2650°F				
		(Cobalt Series)				
283	1.77	10.65	5.40 Co	2.23	3.21	0.50 Co
302	7.17	23.09	5.61 Co	19.47	6.84	1.23 Co
		(Zirconium Series)				
84	0.87	6.34	3.84 Zr	0.06	2.37	0.33 Zr
284	1.09	10.02	6.17 Zr	1.25	2.13	0.84 Zr
300	4.83	23.37	7.44 Zr	21.76	8.02	1.10 Zr
		(Manganese Series)				
85	1.12	6.36	3.64 Mn	0.30	2.08	0.90 Mn
		(Carbon Series)				
87	2.23	6.27	3.33 C	0.85	2.91	---

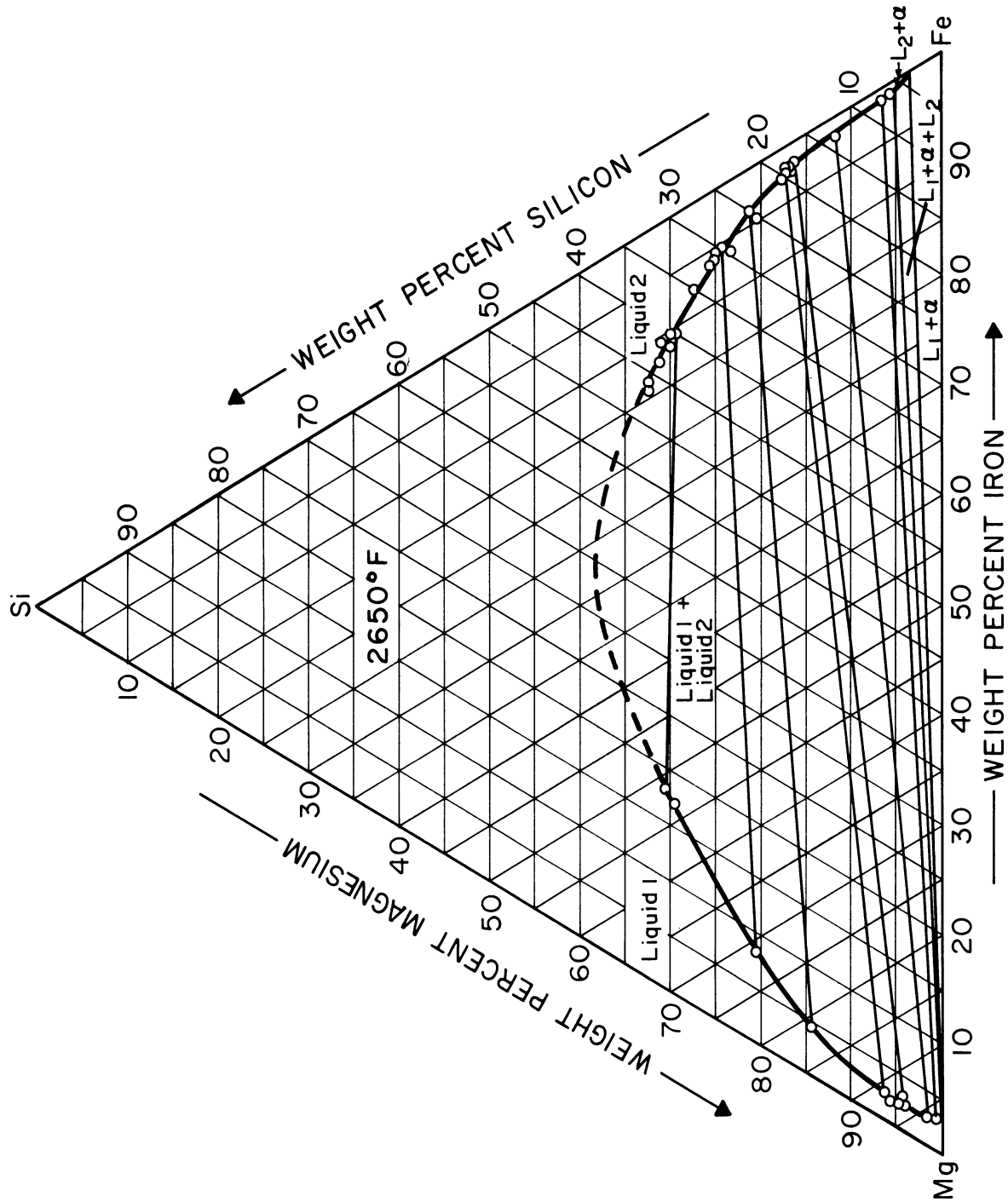

Figure 14. The iron-magnesium-silicon liquid miscibility gap at 2650°F.

polynomial representation of the iron-rich solubility data and a standard deviation of 0.35 percent magnesium for a second-order polynomial representation of the magnesium-rich solubility data.

On the iron-rich side of the liquid miscibility gap, the terminal magnesium solubility is 0.85 percent magnesium at 5.3 percent silicon. The magnesium solubility changes only slightly (0.85 percent to 2.3 percent) as the silicon content increases from 5.3 percent to 17 percent. However, in the range from 17 percent to 34 percent silicon, the magnesium solubility increases from 2.3 percent to 15.2 percent. On the magnesium-rich side of the miscibility gap, the solubility of iron in liquid magnesium at 2650°F is 3 percent. This terminal solubility of iron does not change significantly up to a silicon of 10 percent. Then, in a manner similar to the iron-rich side, the solubility of iron increases markedly as the silicon content is increased.

The tie-lines which extend across the miscibility gap define the respective compositions of equilibrated liquid phases. In a general equilibrated system the tie lines do not have to be parallel nor does the change in their slopes have to indicate that the critical point lies at the summit of the miscibility curve.[26] The tie lines of Figure 14 do indicate slight slope changes with increasing silicon content; however, these slope changes are not wholly in the same direction. The tie-line slopes appear to increase in the initial range up to 15 percent silicon and then decrease as the miscibility envelope becomes smaller. This anomalous behavior is attributed to the marked effect that a small variance in the solubility data at either end of a tie line has on the slope of that tie line. Nevertheless, the general trend shown by these tie

lines indicates that the critical point of the miscibility gap lies near the summit of the curve. The exact determination of the midrange solubility relations cannot be more accurately defined with the present experimental technique. Within this composition range (33-50 %Si), the densities of the two liquid layers become almost identical. Under these conditions representative samples of each liquid phase are difficult to obtain since inductive stirring causes intimate mixing of the two liquids into a suspension.

2. Temperature Effects on Magnesium Solubility

The basic solubility relations have been established at the primary experimental temperature, 2650°F. To determine their temperature dependence, a series of heats were made at 2550°F and 2750°F and two bulk compositions. The results, shown in Figure 15, indicate that changes in temperature have only a minimal effect on the solubility relations.

Of the eight compositions shown in Figure 15, four apparently are within the standard deviation of the basic solubility curves. Additionally, all of these compositions have an inherent uncertainty. Therefore, although these solubility data indicate slight changes in the extent of the miscibility gap as the temperature changes, this effect is minor when compared with the absolute accuracy of the solubility data.

3. Magnesium Vapor Pressure Over the Miscibility Gap

The vapor pressure data obtained over the ternary melts are listed in Table V and are graphically shown in Figure 16. These data can be expressed by the polynomial regression relation:

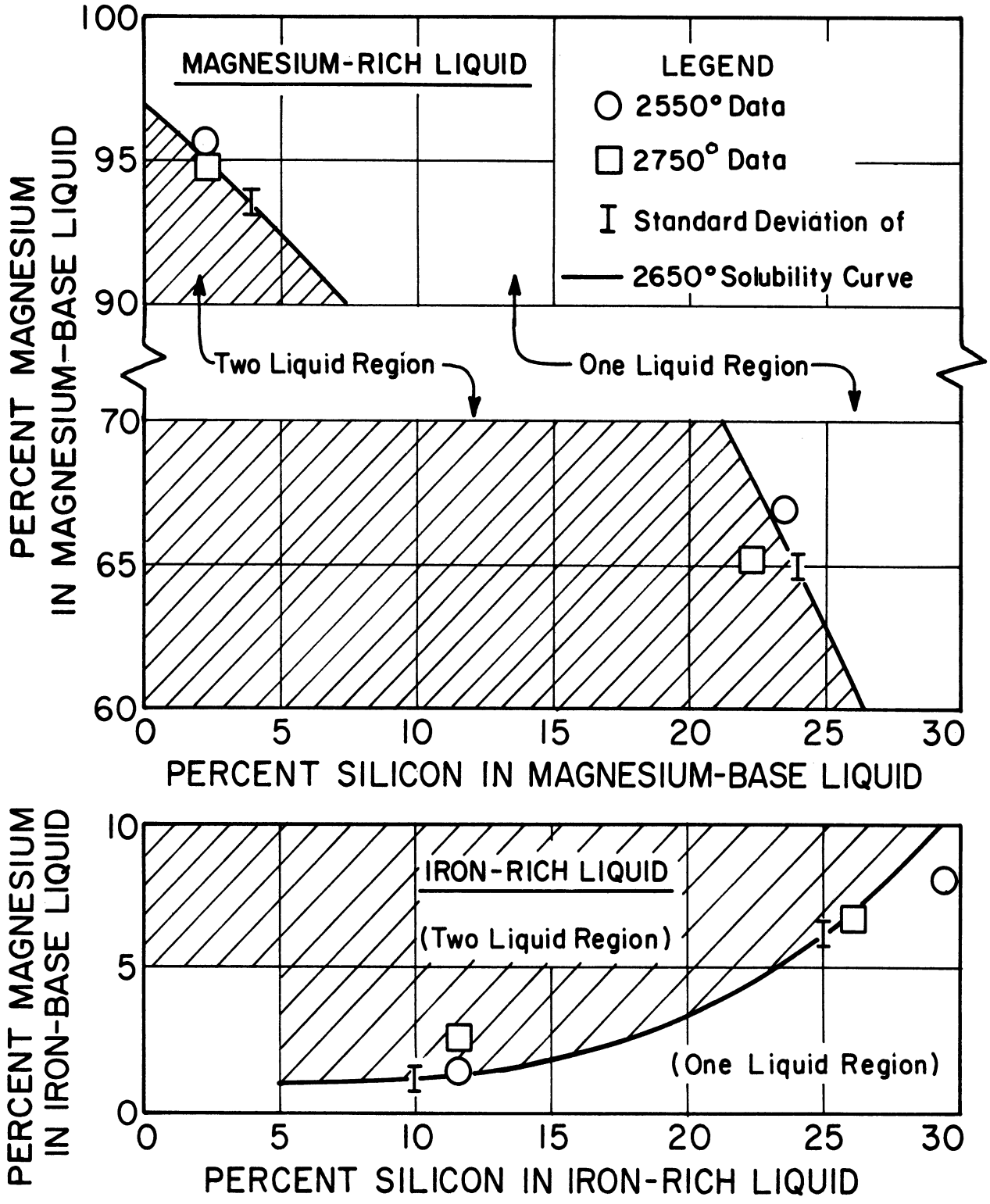

Figure 15. Temperature effect on solubility relations.

TABLE V

VAPOR PRESSURE OF MAGNESIUM IN TERNARY AND QUATERNARY MELTS

Heat No.	Vapor Pressure, psig		Iron-Base Chemistry		
	Melt Data	Vapor Data	%Mg	%Si	%X
		Basic Ternary Data at 2650°F			
179	128	**	1.50*	12.00*	
180	**	74	10.42	30.06	
181	128	128	2.21	17.13	
208	**	100	5.66	24.90	
223	136	137	1.73	11.76	
226	72	76	12.33	31.15	
242	139	**	0.90	5.84	
258	101	101	6.10	25.19	
259	70	**	10.75	30.92	
265	109	107	4.90	20.87	
		Ternary Data at 2550°F			
239	96	95	1.47	11.62	
261	83	73	8.11	29.36	
		Ternary Data at 2750°F			
240	195	200	2.58	11.67	
260	137	130	6.86	26.08	
		Quaternary Data at 2650°F			
		(Cobalt Series)			
283	124	134	1.77	10.65	5.40Co
302	102	108	7.17	23.09	5.61Co
		(Zirconium Series)			
284	**	132	1.09	10.02	6.17Zr
300	99	102	4.83	23.37	7.44Zr

*Calculated from general solubility data.

**Data not taken.

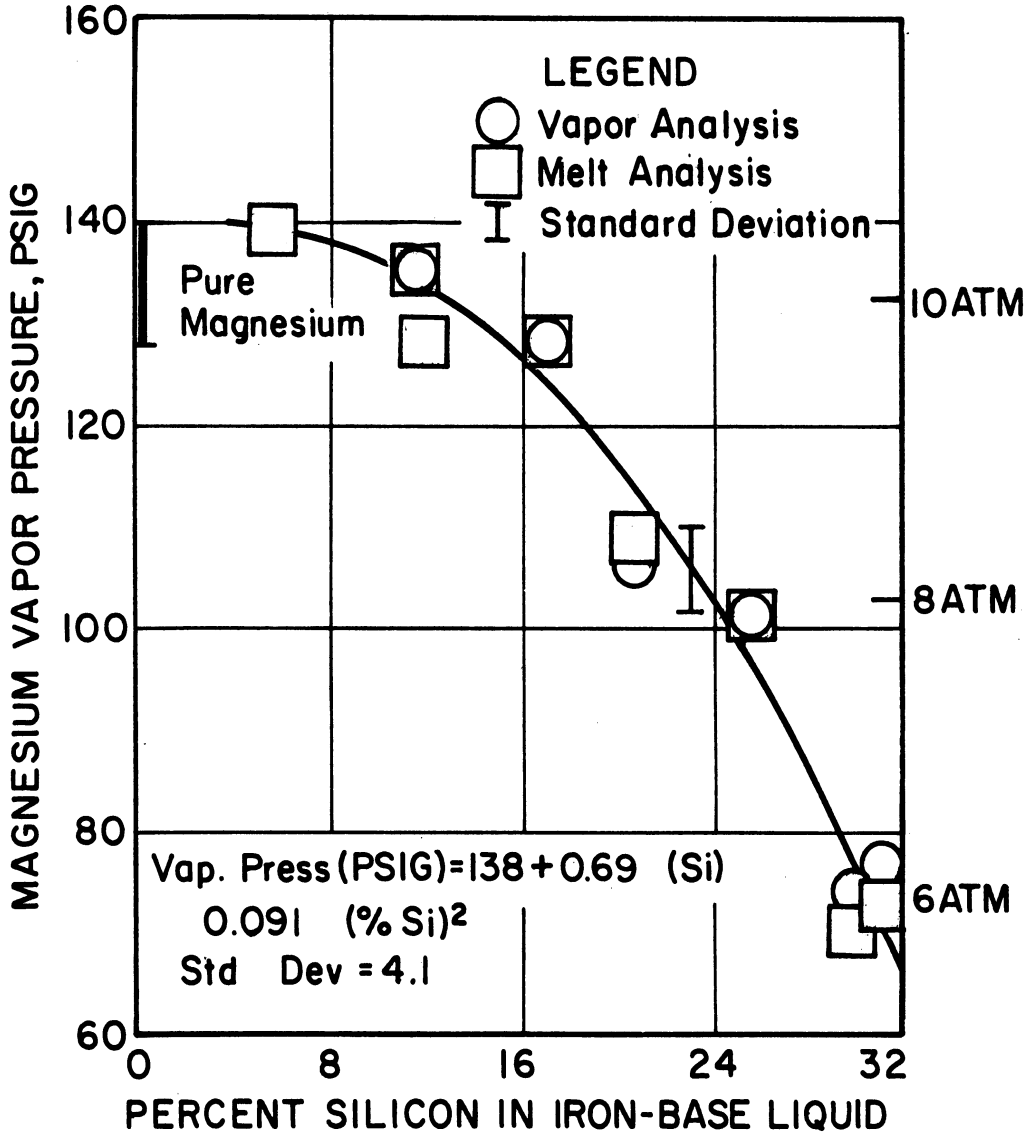

Figure 16. Vapor pressure of magnesium at 2650°F for compositions lying on the ternary immiscibility curve.

$$\text{Vap. Press. Mag. (psig)} = 138 + 0.69\,(\%Si) - 0.09\,(\%Si)^2$$

with a standard deviation of 4 psig.

Over the range of silicon contents from 5 percent to 15 percent, significant changes in the vapor pressure are not indicated. For higher silicon contents, however, the magnesium vapor pressure decreases significantly to a value of 68 psig at a silicon content of 32 percent. This behavior directly

parallels the solubility results which also indicate a marked inflection at about 17 percent silicon.

4. Fourth Element Effects

The effect of additions of several fourth elements on the solubility relations are shown in Figure 17. Although the indicated changes in magnesium solubility are of the same magnitude as the standard deviation, certain trends are evident. At the lower silicon values, additions of carbon and cobalt have the greatest effect on magnesium solubility. Manganese and zirconium additions appear to have only a minor effect; however, the two zirconium compositions investigated both resulted in a slight decrease in the magnesium solubility. At

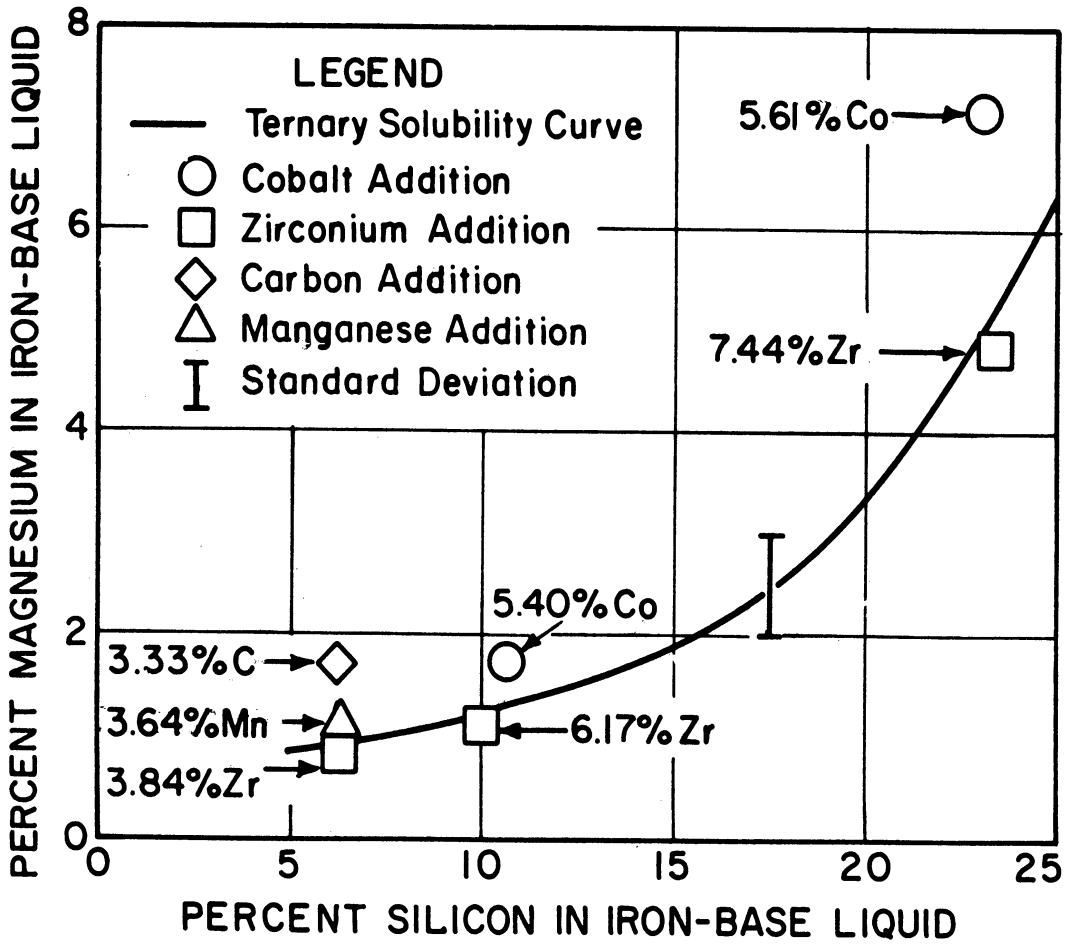

Figure 17. Changes in magnesium solubility with fourth element additions.

the 23 percent silicon level, the cobalt addition of 5.61 percent increases the magnesium solubility by 2.18 percent over the ternary value. Again, the 7.44 percent zirconium addition resulted in a slightly decreased magnesium solubility.

The vapor pressure data obtained for the cobalt and zirconium melts at 10 percent and 23 percent silicon appear to be substantially the same as those data obtained for the ternary melts.

B. THEORETICAL CONSIDERATIONS

An insight into the solution behavior of the two immiscible liquids can be derived from a consideration of the ternary data and the quaternary data. The various implications will be considered first from the standpoint of the solubility relations and then from the standpoint of the vapor pressure data.

1. Implications of the Solubility Data

The two-liquid equilibrium in the Fe-Mg-Si system can be idealized as an iron-rich liquid and a magnesium-rich liquid, both of which are competing for the available silicon. When the system is at equilibrium, the activity of silicon must be the same in both liquid phases. However, if the silicon is attracted more strongly by one of the phases, that phase can show a higher silicon concentration then the other phase.

The ternary phase diagram, redrawn in Figure 18 on an atomic percent basis, shows this competition for the silicon as the slope of the tie lines in the two-liquid region. A more direct representation is shown in Figure 19. Here the silicon partition, defined as

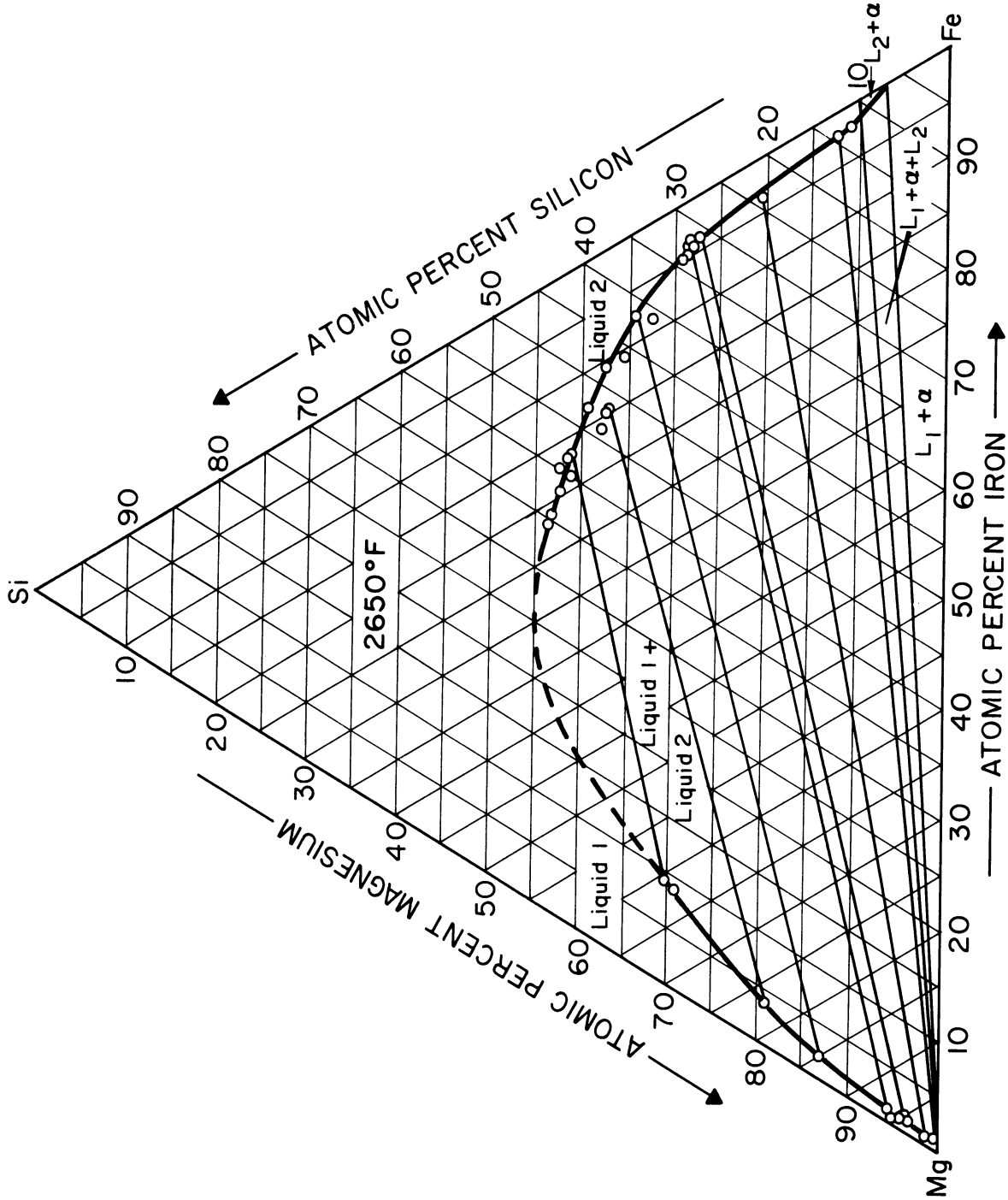

Figure 18. The iron-magnesium-silicon liquid miscibility gap at 2650°F, atomic percent basis.

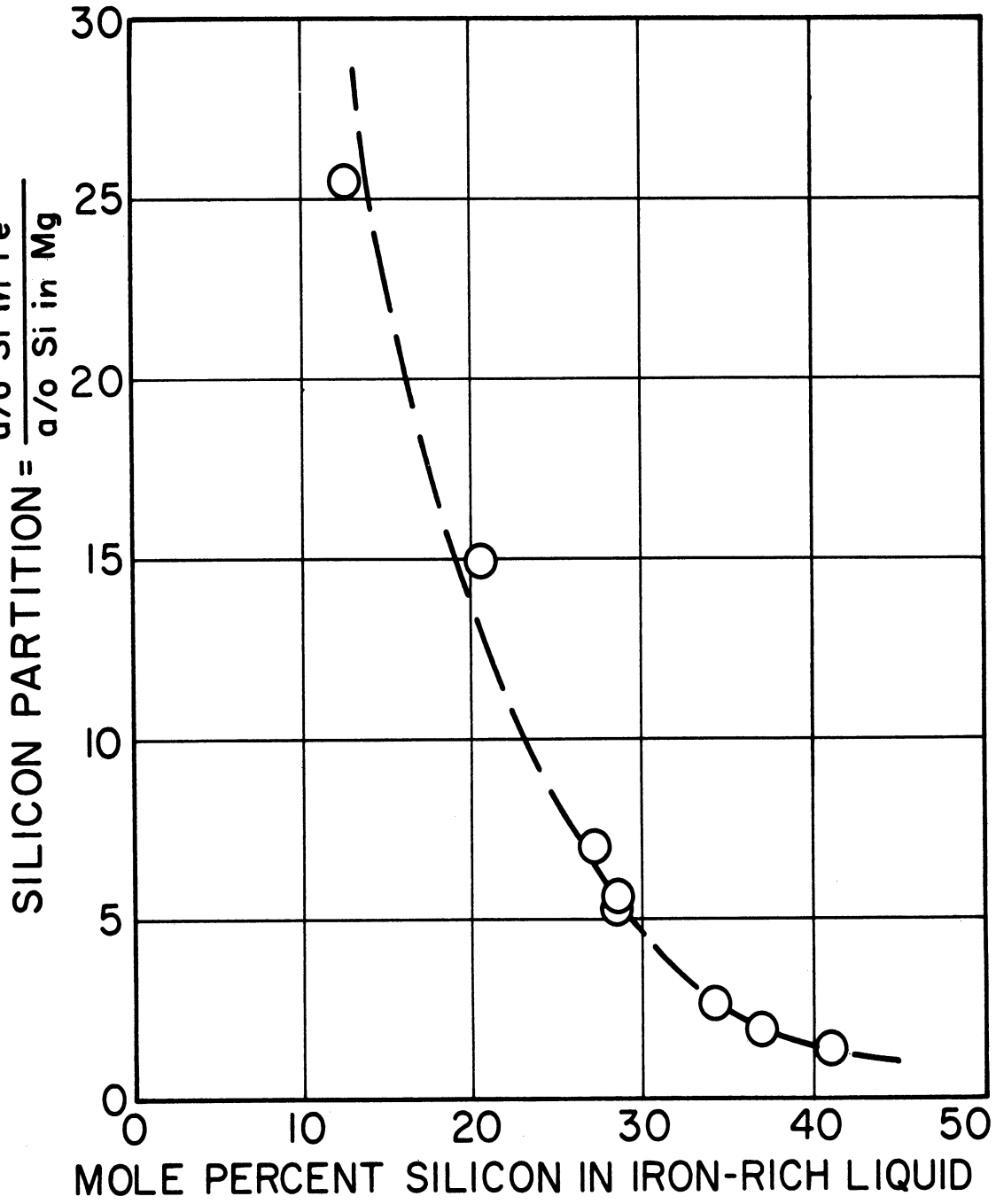

Figure 19. Silicon partition between the immiscible liquid phases at 2650°F.

$$\text{Si partition} = \frac{\text{mole fraction Si in iron-base phase}}{\text{mole fraction Si in magnesium-base phase}},$$

is plotted against the silicon content of the iron-base liquid. At low silicon contents, the silicon partition is quite large, reaching a value of 28 at 12 atomic percent silicon. This high partition value implies a strong tendency toward Fe-Si atomic clustering in the liquid and, correspondingly, a much weaker tendency for Mg-Si atomic clustering. At silicon contents greater than 30 atomic percent, the slope of the partition curve is rapidly decreasing, resulting in relatively low partition values. Correspondingly, the ternary phase diagram, Figure 18, indicates appreciably enhanced magnesium solubility in the iron-rich phase for this range of silicon contents. The increased solubility for magnesium at higher silicon contents may be interpreted either as

(a) the iron and silicon atoms tend to mutually associate thereby reducing the natural repulsion between iron and magnesium atoms, or

(b) the addition of silicon makes the iron-base melt more "silicon-like" thereby reflecting atomic clustering between magnesium and silicon atoms.

Additional evidence for the possibility of atom clustering in the liquid phases can be derived from a consideration of the critical point composition. The silicon partition curve, Figure 19, extrapolates to unity, the critical point, at about 45 atomic percent silicon. The corresponding iron content shown on the ternary diagram, Figure 18, is approximately 20 atomic percent. This composition can also be approximately calculated by considering that at the

critical composition, the liquid structure reflects the two most stable binary silicon compounds Mg_2Si and FeSi. Thus,

Compound	Composition of Compound		
FeSi	20%Fe	20%Si	
Mg_2Si	____	20%Si	40%Mg
Total	20%Fe	40%Si	40%Mg

The solubility data of Figure 18 indicate a somewhat higher silicon content in the critical composition range. This probably reflects a ratio of Mg_2Si to FeSi other than unity, as assumed here.

The addition of a fourth alloying element to an immiscible system of this type presents an even more complex situation. Since, as Klodt[12] points out, the existing theories cannot accurately describe ternary immiscibility phenomena, there is little basis for the prediction of possible relationships in a quaternary. Nevertheless, the data are of some theoretical interest, although they were obtained primarily to determine their possible effects on magnesium solubility and vapor pressure.

The four elements chosen, cobalt, carbon, manganese, and zirconium in conjunction with the ternary elements iron, magnesium, and silicon, exhibit quite different inherent characteristics. However, they can be roughly grouped according to their relative positions in the periodic table, their heats of sublimation, their atomic volumes, and their respective electronegativities. On these bases, cobalt and manganese are elementally similar to iron, carbon is similar to silicon, and zirconium is similar to magnesium.

The changes in magnesium solubility in the iron-rich phase with fourth element additions are shown in Table VI. In general, these changes are not significant in comparison with the calculated standard deviation ($\pm$0.48%Mg) of the ternary data. However, at each major silicon level, a trend is nevertheless evident. The solubility is enhanced by additions of those elements most similar to silicon (carbon) and less significantly by additions of those elements similar to iron (cobalt and manganese). Additions of zirconium resulted in decreased magnesium solubilities.

On the basis of this apparent periodic effect on the solubility changes, various interactions could be hypothesized, such as fourth element substitution for silicon, etc. However, due to the paucity of information available for the six binary systems and four ternary systems which form the basis for any one of these four quaternary systems, any further rationalization would be highly speculative.

2. Implications of the Vapor Pressure Data

The vapor pressure data were obtained for both pure magnesium (Figure 13) and for compositions lying on the ternary immiscibility curve (Figure 16). For data of this type, the thermodynamic activity of magnesium over the ternary miscibility gap is defined as:

$$a_{Mg} = \frac{P_{Mg}}{P^{o}_{Mg}} \qquad (1)$$

where P_{Mg} = vapor pressure of magnesium in the ternary solution

P^{o}_{Mg} = vapor pressure of pure magnesium (standard state is liquid magnesium at the same temperature)

TABLE VI

SOLUBILITY RELATIONS AS AFFECTED BY ADDITION OF FOURTH ELEMENTS

Heat No.:	84	85	87	284	283	300	302
	6% Silicon Level			10% Silicon Level		23% Silicon Level	
Fourth Element:	Zr	Mn	C	Zr	Co	Zr	CO
Iron-Base Liquid							
%Mg*	0.87	1.12	1.70	1.09	1.77	4.83	7.17
%Si	6.34	6.36	6.27	10.02	10.65	23.37	23.09
%X	3.84Zr	3.64 Mn	3.33C	7.17Zr	5.40Co	7.44Zr	5.61Co
Magnesium-Base Liquid							
%Si	0.06	0.30	0.85	1.25	2.23	21.76	19.47
%Fe	2.37	2.08	2.9	2.13	3.21	8.02	6.84
%X	0.33Zr	0.90Mn	---	0.84Zr	0.50Co	1.10Zr	1.23Co
Vap. Press.**	NA	NA	NA	132.3	134.3	100.9	104.2
Ternary Mg-Fe-Si Reference Data (Comparisons based on Si content)							
%Mg in Fe	0.97	0.97	0.97	1.20	1.25	5.18	4.99
Vap. Press.**	139.4	139.4	139.4	136.4	135.8	105.1	106.4
Δ%Mg in Fe	- 0.10	+ 0.15	+ 0.73	- 0.11	- 0.52	- 0.35	+ 2.18
ΔVap. Press	---	---	---	- 4.1	- 1.5	- 4.2	- 2.2

*All compositions on weight percent basis.
**Psig, at 2650°F.

Correspondingly, the activity coefficient of magnesium is defined as

$$\gamma^{x}_{Mg} = \frac{a_{Mg}}{N^{x}_{Mg}} = \frac{P_{Mg}}{N^{x}_{Mg} P^{o}_{Mg}} \qquad (2)$$

where N^{x}_{Mg} = mole fraction magnesium in the x-base ternary liquid.

The activity coefficients of magnesium at 2650°F in the two immiscible liquids are shown in Figure 20. The slight scatter evident in these values is attributed to the variance in the two sets of vapor pressure data. Additionally, calculated values based on silicon partition are used where the magnesium-base liquid composition data is incomplete. Activity coefficients for the data obtained at 2750°F and 2650°F are not included as there are an insufficient amount of data to permit valid conclusions to be drawn.

The magnesium base solutions show ideal solution behavior, as the activity coefficients show only a slight decrease from unity over the range N = 0.98Mg to N = 0.60Mg. This ideal solution behavior over this composition range is required at the higher magnesium contents and is consistent with the high degree of superheat at lower magnesium contents. At lower temperatures the solution behavior is slightly less ideal, as shown by Eldridge, et al.,[8] for the magnesium-silicon system at 1970°F. In direct contrast, the solution of magnesium in the iron-base liquids shows a very strong positive deviation from ideality at low silicon contents. However as the silicon content approaches 0.45 mole percent, the activity coefficient has a value of approximately 2.0, indicating that at higher silicon contents the solution may approach more ideal behavior.

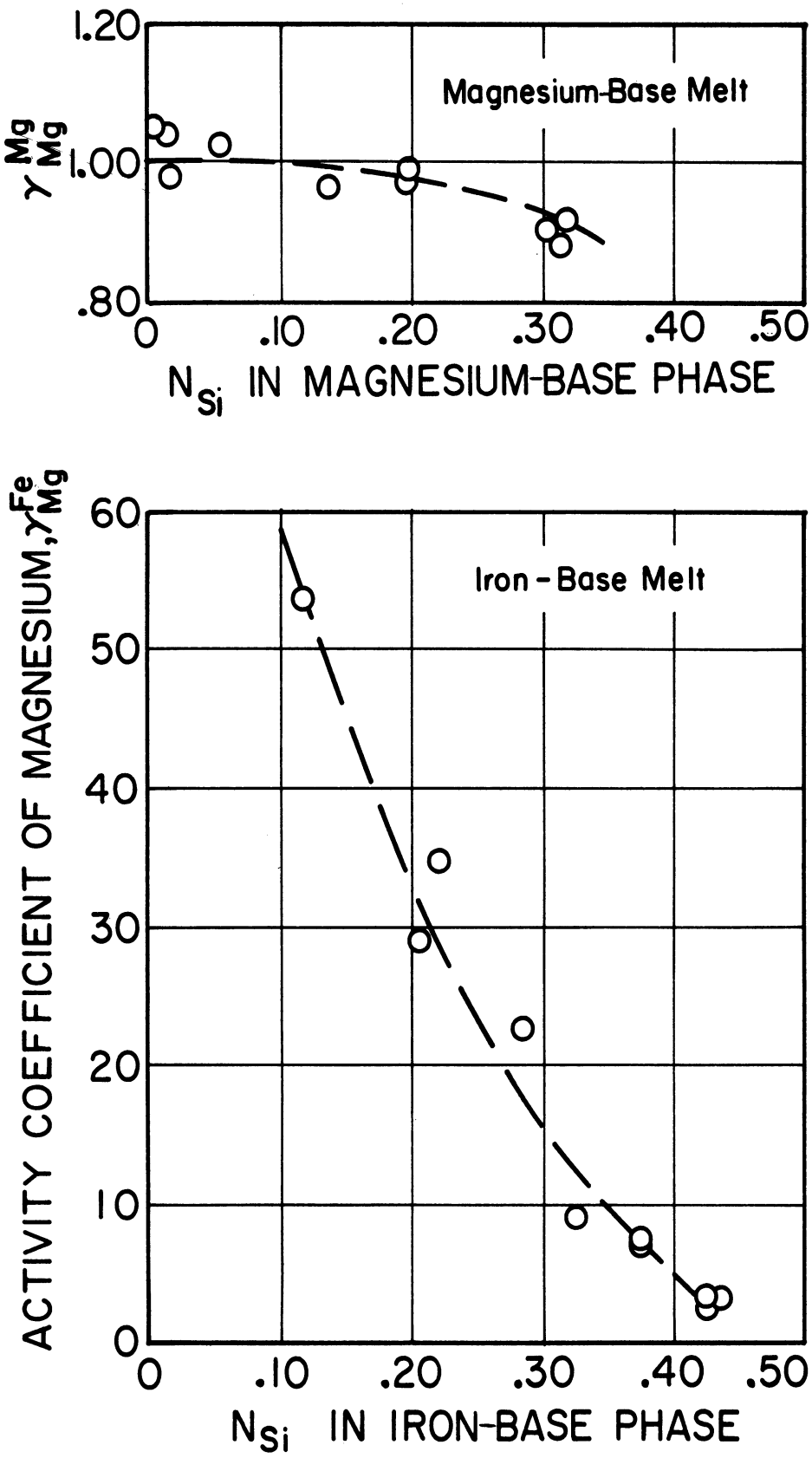

Figure 20. Activity coefficients of magnesium for compositions lying on the immiscibility curve.

These activity coefficient data support the conclusions drawn from the solubility data regarding atomic clustering. The very high activity coefficients of magnesium at low silicon contents in the iron-base liquid are quite consistent with the concept of strong Fe-Si clustering to the almost complete exclusion of magnesium. As the silicon content increases, the activity coefficient decreases, implying increased accommodation for magnesium.

The vapor pressure data from the fourth element heats are shown in Table VI to be not significantly different from the corresponding vapor pressure data for the ternary heats. Therefore, any discussion of fourth element effects relative to changes in the activity coefficient of magnesium revert to the effect that the fourth element addition has on the overall composition, a subject already considered.

C. COMMERCIAL APPLICATIONS

The solubility and vapor pressure data have thus far been discussed as a fundamental addition to the physical chemistry of immiscible liquid metal systems. However, the study was originally suggested by a desire to improve the process for the manufacture of ductile iron through modification of existing magnesium-ferrosilicon alloys. The following discussion, therefore, points out the significance and utilization of these data.

Magnesium ferrosilicon alloys have gained a substantial share of the nodularizing alloy market. They are relatively economical, flexible in regard to addition method, and yield consistent results. Alloy production is accomplished rather easily and economically by adding magnesium to the molten ferrosilicon

product of the submerged arc furnace. The two most important compositions are the 10 percent alloy (8-10%Mg, 45%Si, balance Fe) and the 5 percent alloy (5%Mg, 45%Si, balance Fe). Although minor amounts of cerium and calcium may also be present, the major constituents are thus seen to be the same as those of the ductile cast iron product.

Nevertheless, these alloys also possess certain characteristics which handicap their more widespread use. The most troublesome handicap is the high silicon to magnesium ratios of these alloys, which range from 4.5 to 9.0. Magnesium additions generally constitute about 0.20 lb of magnesium per 100 lb of molten iron. Associated with this magnesium addition is the addition of 0.9 to 1.8 lb of silicon, or a corresponding increase in the silicon content of the ductile iron product of over 1 percent. A silicon pick-up of this magnitude is considered excessive for many operations. Another handicap is the low density of the solid alloy (3.8-4.5 gm/cc) as compared to that of molten cast iron (6.60 gm/cc). Thus if the alloy addition is not mechanically entrapped as in the plunging process, it will readily rise to the surface where the magnesium will burn and be lost.

A superior magnesium ferrosilicon alloy would thus be one which has a higher density, a lower silicon content, and a lower magnesium vapor pressure than the present alloy, but which is still economically comparable. Since silicon is a light element and since silicon pick-up is objectionable, replacement of silicon by iron shows some potential. However, this replacement would result in an increased magnesium vapor pressure, based on the results shown in preceding sections. Correspondingly, the present alloy manufacturing process

is relatively unsophisticated. If a major processing change is dictated, the relative economics could be quite drastically affected. Therefore, an optimization of the above considerations is required.

The preceding equilibrium results represent most of the information basic to composition optimization. The ternary miscibility curve, Figure 14, indicates the limiting magnesium contents which can be attained at silicon contents less than 35 percent. Magnesium vapor pressure values for these limiting compositions are shown in Figure 16. The effect of fourth element additions on the solubility and vapor pressure relations is shown in Tables IV and V.

To provide a reasonable estimate of the density values which can be obtained at various silicon contents, density measurements were made on the iron base portion of selected ingots from this investigation. The results, shown in Figure 21, indicate that at the lower silicon levels, a density almost twice that of the current commercial alloys can be attained.

Additional information for composition optimization is derived from consideration of the solidification characteristics of the various compositions. As mentioned previously, the melt thermocouple, which extends up into the crucible, is sensitive to temperature changes. It is thus possible to record the cooling inflections evidenced by the melt after the sampling operation has been completed. It should be pointed out that the basic experimental design was dictated by the desire to obtain immiscibility relationships. The use of the melt thermocouple to record cooling inflections was not meant to represent an optimum technique for the determination of the crystallization of these alloys. On the other hand, the very existence of several inflections in the

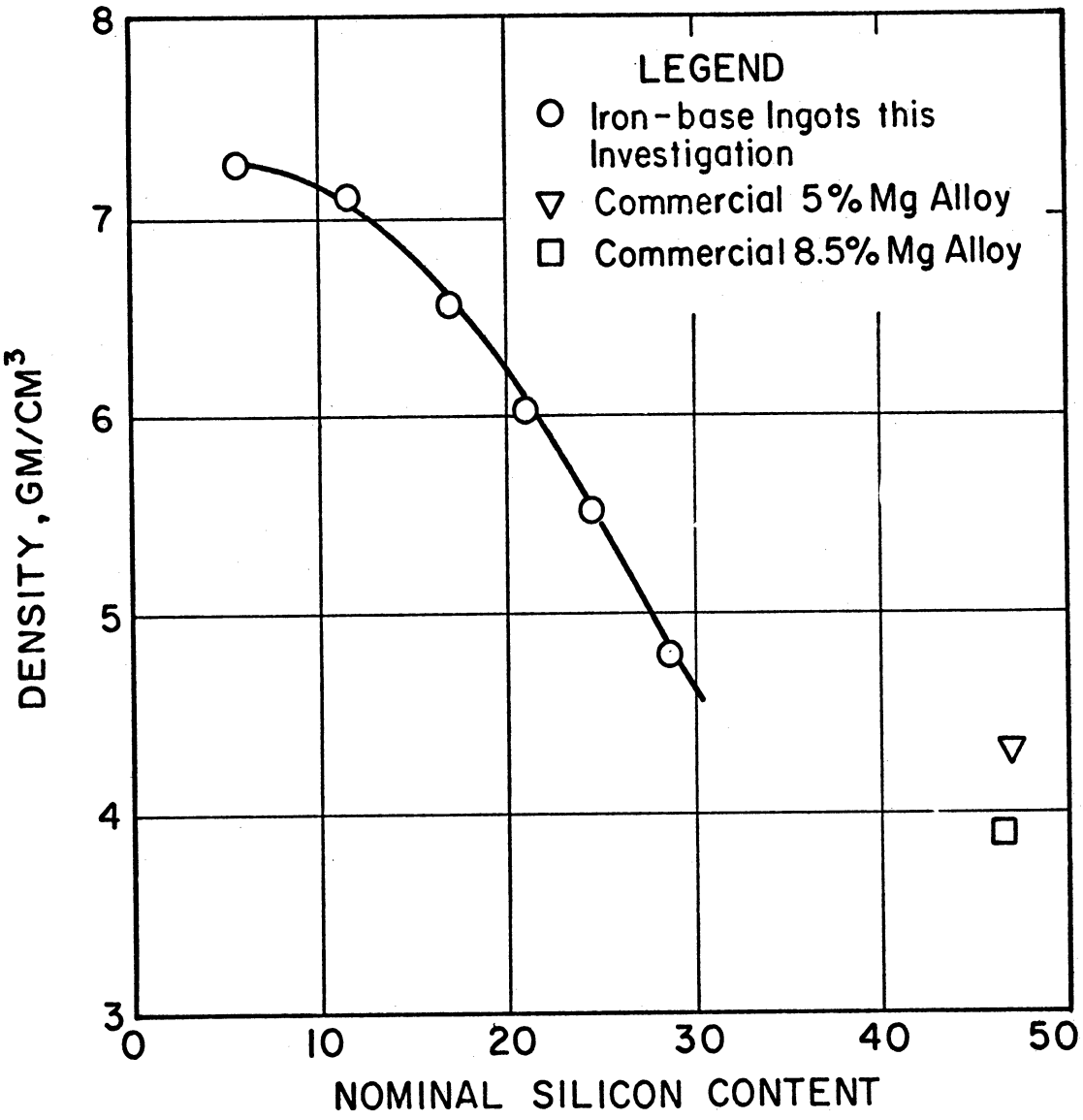

Figure 21. Density of iron-rich portion of ingots from this investigation.

cooling curves would suggest crystallization relationships which are dependent upon the alloy chemistry. The following discussion, therefore, attempts to rationalize these changes in crystallization as recorded by a technique considered not to be the most desirable for this application.

Cooling inflections evidenced by a series of alloys with varying silicon contents are shown in Table VII together with a description of the phases present in the solidified ingots. These phase determinations were made on

TABLE VII

SOLIDIFICATION BEHAVIOR OF COMPOSITIONS LYING ON THE TERNARY IMMISCIBILITY CURVE

Heat No.	Composition				Temperature of Cooling Curve Inflections					Primary Solid Phase	Other Phases[2]
	Iron Base		Mag. Base								
	%Mg	%Si	%Si	%Fe	1	2	3	4	5		
242	.90	5.84	.60	1.91	2545	2450	2315	2210		Iron-Fe[1] Mag.-Mg	Iron-Mg Mag.-Mg_2Si, Fe
223	1.73	11.76	1.56	2.64	2510	2300	2277	2250	2209	Iron-Fe Mag.-eut. $Mg+Mg_2Si$	Iron-Mg Mag.-Fe, FeSi
181	2.21	17.13	6.10	2.66	2375	2202	2128	2097	1944	Iron-Fe Mag.-Mg_2Si	Iron-Mg, FeSi, Mg_2Si Mag.-Mg, FeSi, Fe
280	3.87	21.18	4.43	4.47	2335	2220	2095	1935		Iron-FeSi Mag.-Mg_2Si	Iron-Fe, Mg_2Si, Mg Mag.-Mg, FeSi, Fe
279	5.64	24.57	20.47	8.26	2350	2290	2225	2095	1935	Iron-FeSi Mag.-Mg_2Si	Iron-Fe, Mg_2Si, Mg Mag.-FeSi, Mg, Fe
278	10.43	29.56	30.38	17.94	2380	2220	2080	1935		Iron-FeSi Mag.-Mg_2Si	Iron-Mg_2Si, Fe, Mg Mag.-FeSi, Mg, Fe

(1) Fe-iron saturated with silicon.

(2) Listed in approximate order of amount present.

polished and etched samples using reflected and polarized light to identify the phases on the basis of color, shape, and etching characteristics. No indications of the presence of the $FeSi_2$ compound were detected, even at the highest silicon content studied.

All of this basic information then can be used both to predict the behavior of various compositions when applied as a nodularizing agent to produce ductile cast iron and also to predict some of the manufacturing parameters. The results of some sample calculations are shown in Tables VIII and IX. These results can best be discussed by noting the implications over various ranges of silicon contents and comparing these with comparable results for current alloys.

The compositions low in silicon content (5, 10, and 25 percent silicon) are characterized by low saturated magnesium contents, comparatively high vapor pressures, and high densities. For low saturated magnesium contents, the magnesium recovery after addition to a cast iron melt should be quite high, as shown by the results of Clark and McCluhan.[4] Their data show an inverse parabolic relationship between magnesium recovery and the magnesium content of the treatment alloy. Thus, since less magnesium has to be used, the amount of silicon also added is reasonably low, in spite of the comparatively high silicon-to-magnesium ratios. A factor which could limit the application of these compositions is the amount of alloy which must be added to ensure an adequate residual magnesium content. As shown in Table VIII, a quantity about twice that for current alloys would have to be added. The resulting thermal losses could conceivably be too high. However, these calculations show that the application of these compositions as nodularizing alloys is feasible.

TABLE VIII

CALCULATED NODULARIZING PROPERTIES OF SATURATED Mg-Fe-Si ALLOYS

Nominal Si Level	Sat'd Mg Content	Net Density, gm/cc	Vapor Press., psig (1)	Alloy Si/Mg Ratio	Assumed Mg Recovery (2)	Lb Alloy for .04%Mg in 100 lb (3)	Lb Si Added in 100 lb (4)
5	0.95	7.22	134	6.3	80%	5.26	.26
10	1.20	7.15	134	8.3	70%	4.76	.48
15	1.75	6.85	127	8.6	57%	4.01	.60
20	3.40	6.20	116	5.9	37%	3.18	.64
25	6.45	5.45	100	3.9	24%	2.58	.65
30	10.60	4.70	77	2.8	18%	2.10	.63
Reference Data for Current Alloys(2)							
45.0	5.0	4.30	(5)	9.0	29%	2.76	1.24
45.0	9.0	3.90	(5)	5.0	20%	2.22	1.00

(1) At 2650°F equilibrium conditions.

(2) Reference 4.

(3) $$\text{Lb alloy} = \frac{(100)(0.04)}{(\frac{\%\ \text{recovery}}{100})(\frac{\%\text{Mg in}}{\text{alloy}})}.$$

(4) $$\text{Lb Si} = (\text{lb alloy})(\frac{\%\text{Si in alloy}}{100}).$$

(5) Less than one atmosphere at 2600°F (0 psig).

TABLE IX

CALCULATED MANUFACTURING PARAMETERS OF SATURATED Mg-Fe-Si ALLOYS

Nominal Si Level	Sat'd Mg Content	Liquidus Temp., °F	Vapor Press. at Liquidus, psig	Net Density, lb/ft^3	Lb Mg per ft^3 Alloy	Balanced Charge Composition* for 100 lb of Mg-Fe-Si Alloy		
						Lb 50%FeSi	Lb Fe	Lb Mg
5	0.95	2540	95	450	4.3	10	89.0	.95
10	1.20	2510	85	446	5.4	20	78.8	1.20
15	1.75	2375	60	428	7.5	30	68.25	1.75
20	3.40	2335	32	386	13.1	40	56.6	3.40
25	6.45	2350	25	340	21.9	50	43.55	6.45
30	10.60	2380	25	293	31.1	60	29.40	10.60
45	5.0	2375	**	268	13.4	90	5.0	5.0
45	9.0	2275	**	243	21.9	90	1.0	9.0

*Assumes 100% recovery of all additions.
**Less than 1 atmosphere (0 psig).

The calculated manufacturing parameters shown in Table IX indicate that the production of such compositions may not be entirely feasible. The liquidus temperatures and the magnesium activities are quite high; thus, the vapor pressure at the melting point varies from 5 to 7.5 atmospheres. This imposes rather severe restrictions on furnace design and operations. Additionally, if the material input of molten 50 percent ferrosilicon, cold steel scrap and magnesium ingot is assumed, the dilutions would be so severe that a melting step would be necessitated. A process incorporating an entirely cold charge and a complete melting procedure might be more practical. In any event, the associated manufacturing costs would probably be excessive in comparison with the present process.

The intermediate compositions with silicon contents of from 20 percent to 30 percent show a better balance of properties, as shown in Table VIII. The densities are still considerably better than those of the current alloys, the vapor pressures are more reasonable as the magnesium activity is lower, and the silicon-to-magnesium ratios are quite low. Since the saturated magnesium contents are considerably higher than for the lower silicon alloys, the magnesium recoveries should be consequently lower, as predicted again by the results of Clark and McCluhan.[4] However, the silicon pick-up of a treated bath would be reasonably low, since the silicon-to-magnesium ratios are low. Additionally, the amount of alloy addition required is less than for the lower silicon alloys, so the temperature loss of a melt would be expected to be lower after the treatment process. Thus the application of compositions over this range of silicon contents appears to be entirely feasible.

Referring to Table IX, the production of these compositions also appears to be more practicable than for the lower silicon alloy. Since both the liquidus temperatures and the magnesium activities are lower, the vapor pressures at the melting points range from about 2.7 atmospheres to 3.2 atmospheres. Suitable pressure furnace designs for this pressure range would be less sophisticated and consequently less costly. Additionally, the amount of magnesium per cubic foot of alloy is almost an order of magnitude greater than for the lower silicon alloys, thus increasing the possible furnace throughput. However, charge calculations similar to those shown previously indicate that a melting step would be necessitated, thus increasing the complexity of the process.

The optimum composition range appears to be 20 percent to 25 percent silicon with associated saturated magnesium contents of from 3.4 percent to 6.5 percent. Such an alloy composition would be capable of achieving proper ductile iron treatment at a reasonable magnesium efficiency with a minimum amount of silicon pick-up. Although the production cost would undoubtedly be higher than the current alloy production cost, the density and the contained magnesium per cubic foot of alloy would be higher than the current alloys.

There is one additional factor which might be considered. If the magnesium content is lowered while keeping the iron-to-silicon ratio constant, the vapor pressure would also correspondingly decrease. This enhanced property would have to be weighed against the associated increase in the magnesium-to-silicon ratio which could be significant if the magnesium recovery did not increase proportionally. It is conceivable, however, that practical production

limitations might favor compositions which do not approach imminent immiscibility. These considerations should become more evident as further development transpires.

The data shown for the influence of fourth element additions indicated only minimal effects on solubility and vapor pressure. Therefore, for the elements investigated (Co, Mn, Zr, C) and conceivably for other similar elements, the possible benefits which could be achieved would seem to be chiefly economic. However, under current conditions, the relative low cost of silicon would negate any such promise.

The results of this investigation thus show that new composition ranges for magnesium-ferrosilicon alloys are technically feasible, both for application and production. Future optimization of composition limits will be required in order to develop these alloys for commercial application and to evaluate the economic variables. It is felt the best solution to the alloy and economic development problems can now be most readily accomplished by Union Carbide Corporation.

V. CONCLUSIONS

The following conclusions may be drawn from the results of the present investigation:

1. A technique for the determination of vapor pressures in excess of one atmosphere has been developed which can be applied to other systems with one highly volatile component. The validity of the technique has been verified by determining magnesium vapor pressures over a range from 3 atmospheres to 15 atmospheres.
2. A crucible design and a sampling technique have been developed which are suitable for future investigations with corrosive high temperature metallic liquids.
3. The liquid miscibility gap in the iron-magnesium-silicon system at 2650°F can be divided into three regions for the iron-base liquid; an initial region where the magnesium solubility in the iron phase increases from 1 percent to 2.5 percent as the silicon content increases from 5 percent to 18 percent, a rapidly changing region where the magnesium solubility further increases to 14 percent at a silicon content of 33 percent, and the critical composition region (35 to 40 percent silicon) where the miscibility gap is closed. The corresponding iron solubility regions in the magnesium-rich liquid for these levels are: 3 percent at zero silicon, 3 percent at 10 percent silicon, and 21.5 percent at 33 percent silicon.
4. The vapor pressure of magnesium over the ternary liquid at 2650°F is

approximately 134 psig for silicon contents up to 16 percent. At higher silicon contents the vapor pressure decreases significantly reaching a value of 68 psig at 32 percent silicon.

5. The fourth element additions investigated (cobalt, manganese, carbon zirconium) had only a minor effect on solubility and vapor pressure relations.

6. These data provide the necessary information for further development of iron-magnesium-silicon addition alloys through optimization of magnesium content and density.

7. In the iron-magnesium-silicon system, the solubility phenomena can be rationalized on the basis of interaction between the elemental species.

Several subjects deserving future work are suggested by this investigation. These include:

1. Utilization of the vapor pressure technique in the single phase areas to describe the iso-activity curves,

2. a similar investigation of systems such as iron-magnesium (transition element) which might be less interactive to further delineate the theoretical aspects of liquid metal immiscibility at high temperature, and,

3. an intensive investigation at several bulk compositions of the effect of fourth elements on solubility relations.

APPENDIX I

CHEMICAL ANALYSIS TECHNIQUES

The following general analytical procedures, specially adapted to this investigation, were used.

A. IRON BASE SAMPLE ANALYSIS

1. Silicon Determination

The crushed sample is fused with Na_2O_2, the fusion is dissolved in HCl, and the SiO_2 is dehydrated with $HClO_4$. (In the case of high SiO_2, a double dehydration is made.) The resultant silica precipitate is then filtered, ignited, and weighed. Finally, the SiO_2 is volatilized with HF and $H_2 \cdot SO_4$ and the $\%SiO_2$ calculated.

2. Magnesium Determination

The crushed sample is first treated with concentrated HNO_3 on a dry platinum casserole with a dropwise addition of HF. Next, $HClO_4$ is added and the solution is evaporated to fumes. Lanthanum chloride is added to an aliquot of this solution and the magnesium content is determined by Atomic Absorption Spectroscopy.

B. MAGNESIUM BASE SAMPLE ANALYSIS

1. Silicon Determination

The crushed sample is first treated with concentrated HNO_3 in a dry cas-

serole. Then $HClO_4$ is added and heated until the $HClO_4$ fumes. After cooling, water is added, and the solution is filtered. The filtrate is reserved. The filtered residue is ignited to oxides in Vycor. These cooled oxides are then brushed into an iron crucible for fusion with Na_2O_2. The subsequent cooled fusion is combined with the reserved filtrate. From this point the silicon determination follows that for the iron base material.

2. Iron Determination

The crushed sample is first dissolved in a dry, platinum dish with HNO_3, HF, and $HClO_4$. This solution is then taken to fumes of $HClO_4$, cooled and transferred to a Pyrex beaker where it is ammoniated, boiled, and filtered. The $Fe(OH)_3$ is dissolved in HCl and boiled. The iron is reduced with $SnCl_2$ and oxidized with titrated $K_2Cr_2O_7$ in the Zimmermann-Reinhardt reaction.

APPENDIX II

VAPOR PRESSURE ANALYSIS PROGRAM

The program for analysis of vapor pressure data uses a standard linear regression calculation to yield a best-fit line, the standard error of the data about that line, and the correlation coefficient. The calculated results are then used to determine vapor pressure values at selected temperatures from 2000°F to 3000°F.

The data illustrated here comprise all of the vapor pressure data obtained in this investigation for pure magnesium. Similar calculations were made for all ternary and quaternary heats that yielded suitable melt temperature data. The correlation of the melt temperature data was then checked against the vapor temperature determination to provide an estimate of the accuracy of the data.

VAPOR PRESSURE ANALYSIS PROGRAM

23 AUG 68 VERSION

FOLLOWING ARE THE RESULTS OF A REGRESSION ANALYSIS USING SUBROUTINE LINREG. THE RESULT IS AN EQUATION OF THE FORM

Y = A + B*X

WHERE Y= LOG OF PRESSURE IN ATMOSPHERES
X= RECIPROCAL TEMPERATURE (10000/DEGREES RANKINE)

THE EXPERIMENTAL DATA TO BE ANALYZED FOLLOW

TEMPERATURE		PRESSURE	
DEG F	DEG R	PSIA	ATM
2290.0	2749.70	44.7	3.04
2305.0	2764.70	44.7	3.04
2315.0	2774.70	49.7	3.38
2330.0	2789.70	54.7	3.72
2390.0	2849.70	64.7	4.40
2410.0	2869.70	74.7	5.08
2445.0	2904.70	84.7	5.76
2480.0	2939.70	89.7	6.10
2525.0	2984.70	99.7	6.78
2550.0	3009.70	114.7	7.80
2610.0	3069.70	124.7	8.48
2622.0	3081.70	134.7	9.16
2622.0	3081.70	134.7	9.16
2640.0	3099.70	134.7	9.16
2645.0	3104.70	144.7	9.84
2720.0	3179.70	169.7	11.54
2740.0	3199.70	194.7	13.24
2745.0	3204.70	194.7	13.24
2760.0	3219.70	204.7	13.93
2760.0	3219.70	204.7	13.93
2772.0	3231.70	214.7	14.61
2775.0	3234.70	214.7	14.61
2792.0	3251.70	224.7	15.29
2792.0	3251.70	224.7	15.29

RESULTS

THE EQUATION OBTAINED IS --

LOGP = (4.92797) + (-1.21995) * 10000/T

STANDARD ERROR OF ESTIMATE = 0.01320

CORRELATION COEFFICIENT = 0.99839

THE RESULTS WHICH FOLLOW ARE OBTAINED USING THE INDICATED TEMPERATURES IN THE ABOVE EQUATION.

TEMPERATURE			PRESSURE	
DEG F	DEG R	10000/DEG R	LOG P	PSI A
2000.00	2459.70	4.0655	-0.0318	13.66
2010.00	2469.70	4.0491	-0.0117	14.31
2020.00	2479.70	4.0327	0.0082	14.98
2030.00	2489.70	4.0165	0.0280	15.68
2040.00	2499.70	4.0005	0.0476	16.40
2050.00	2509.70	3.9845	0.0670	17.15
2060.00	2519.70	3.9687	0.0863	17.93
2070.00	2529.70	3.9530	0.1055	18.74
2080.00	2539.70	3.9375	0.1244	19.58
2090.00	2549.70	3.9220	0.1433	20.45
2100.00	2559.70	3.9067	0.1620	21.34
2110.00	2569.70	3.8915	0.1805	22.28
2120.00	2579.70	3.8764	0.1989	23.24
2130.00	2589.70	3.8615	0.2172	24.24
2140.00	2599.70	3.8466	0.2353	25.27
2150.00	2609.70	3.8319	0.2533	26.34
2160.00	2619.70	3.8172	0.2711	27.44
2170.00	2629.70	3.8027	0.2888	28.59
2180.00	2639.70	3.7883	0.3064	29.77
2190.00	2649.70	3.7740	0.3239	30.99
2200.00	2659.70	3.7598	0.3412	32.25
2210.00	2669.70	3.7457	0.3583	33.55
2220.00	2679.70	3.7318	0.3754	34.89
2230.00	2689.70	3.7179	0.3923	36.28
2240.00	2699.70	3.7041	0.4091	37.71
2250.00	2709.70	3.6904	0.4258	39.19
2260.00	2719.70	3.6769	0.4424	40.71
2270.00	2729.70	3.6634	0.4588	42.28
2280.00	2739.70	3.6500	0.4751	43.90
2290.00	2749.70	3.6368	0.4913	45.56
2300.00	2759.70	3.6236	0.5074	47.28
2310.00	2769.70	3.6105	0.5233	49.05
2320.00	2779.70	3.5975	0.5392	50.87
2330.00	2789.70	3.5846	0.5549	52.75
2340.00	2799.70	3.5718	0.5705	54.68
2350.00	2809.70	3.5591	0.5860	56.67
2360.00	2819.70	3.5465	0.6014	58.72
2370.00	2829.70	3.5339	0.6167	60.82
2380.00	2839.70	3.5215	0.6319	62.98
2390.00	2849.70	3.5091	0.6470	65.21
2400.00	2859.70	3.4969	0.6620	67.50
2410.00	2869.70	3.4847	0.6768	69.85
2420.00	2879.70	3.4726	0.6916	72.26
2430.00	2889.70	3.4606	0.7062	74.74
2440.00	2899.70	3.4486	0.7208	77.29
2450.00	2909.70	3.4368	0.7353	79.91
2460.00	2919.70	3.4250	0.7496	82.59
2470.00	2929.70	3.4133	0.7639	85.35
2480.00	2939.70	3.4017	0.7780	88.18
2490.00	2949.70	3.3902	0.7921	91.08

TEMPERATURE			PRESSURE	
DEG F	DEG R	10000/DEG R	LOG P	PSIA
2500.00	2959.70	3.3787	0.8061	94.06
2510.00	2969.70	3.3673	0.8200	97.12
2520.00	2979.70	3.3560	0.8338	100.25
2530.00	2989.70	3.3448	0.8475	103.46
2540.00	2999.70	3.3337	0.8611	106.75
2550.00	3009.70	3.3226	0.8746	110.13
2560.00	3019.70	3.3116	0.8880	113.58
2570.00	3029.70	3.3007	0.9013	117.12
2580.00	3039.70	3.2898	0.9146	120.75
2590.00	3049.70	3.2790	0.9277	124.47
2600.00	3059.70	3.2683	0.9408	128.27
2610.00	3069.70	3.2576	0.9538	132.16
2620.00	3079.70	3.2471	0.9667	136.15
2630.00	3089.70	3.2366	0.9795	140.23
2640.00	3099.70	3.2261	0.9923	144.40
2650.00	3109.70	3.2157	1.0049	148.67
2660.00	3119.70	3.2054	1.0175	153.04
2670.00	3129.70	3.1952	1.0300	157.51
2680.00	3139.70	3.1850	1.0424	162.08
2690.00	3149.70	3.1749	1.0547	166.75
2700.00	3159.70	3.1649	1.0670	171.52
2710.00	3169.70	3.1549	1.0792	176.40
2720.00	3179.70	3.1449	1.0913	181.38
2730.00	3189.70	3.1351	1.1033	186.48
2740.00	3199.70	3.1253	1.1153	191.68
2750.00	3209.70	3.1156	1.1271	197.00
2760.00	3219.70	3.1059	1.1389	202.42
2770.00	3229.70	3.0963	1.1507	207.97
2780.00	3239.70	3.0867	1.1623	213.63
2790.00	3249.70	3.0772	1.1739	219.40
2800.00	3259.70	3.0678	1.1854	225.30
2810.00	3269.70	3.0584	1.1969	231.32
2820.00	3279.70	3.0491	1.2083	237.45
2830.00	3289.70	3.0398	1.2196	243.72
2840.00	3299.70	3.0306	1.2308	250.11
2850.00	3309.70	3.0214	1.2420	256.62
2860.00	3319.70	3.0123	1.2531	263.27
2870.00	3329.70	3.0033	1.2641	270.05
2880.00	3339.70	2.9943	1.2751	276.95
2890.00	3349.70	2.9853	1.2860	284.00
2900.00	3359.70	2.9765	1.2968	291.17
2910.00	3369.70	2.9676	1.3076	298.49
2920.00	3379.70	2.9588	1.3183	305.94
2930.00	3389.70	2.9501	1.3290	313.54
2940.00	3399.70	2.9414	1.3396	321.27
2950.00	3409.70	2.9328	1.3501	329.15
2960.00	3419.70	2.9242	1.3605	337.18
2970.00	3429.70	2.9157	1.3709	345.35
2980.00	3439.70	2.9072	1.3813	353.68
2990.00	3449.70	2.8988	1.3916	362.15
3000.00	3459.70	2.8904	1.4018	370.77

APPENDIX III

SOLUBILITY DATA ANALYSIS PROGRAM

The program for analysis of the solubility data used a standard nth order polynominal regression calculation. First through fifth order polynominal curves are fit to the input data and the standard deviation of the points about these curves is calculated. Equilibrium magnesium solubilities are also calculated for each curve at integral silicon contents from 1 to 40 percent.

Two sets of solubility data are shown in this appendix. The first set comprises the iron-rich compositions and the second set is the magnesium-rich compositions. A fourth-order regression polynomial was judged to fit the iron-rich data most satisfactorily and a second-order regression polynomial was judged to best represent the magnesium-rich data. These judgements were based on the relative values of the standard deviations and the characteristics of the plotted curves. The calculated compositions for the two most representative polynominals were used to plot the ternary curves in Figure 14 and for comparative purposes in the succeeding analyses.

SOLUBILITY DATA ANALYSIS PROGRAM

FOLLOWING ARE THE INPUT AND RESULTS OF A REGRESSION ANALYSIS PROGRAM WHICH ANALYZES SOLUBILITY DATA USING 5 POLYNOMIALS FROM FIRST THROUGH FIFTH ORDER INCLUSIVE

THE RESULTS ARE PRESENTED AS AN EQUATION EXPRESSING THE EQUILIBRIUM MAGNESIUM CONTENT AS A POLYNOMIAL FUNCTION OF SILICON CONTENT.

THE EXPERIMENTAL DATA TO BE ANALYZED FOLLOW:

HEAT	PCT. MG	PCT. SI	HEAT	PCT. MG	PCT. SI
82	0.97	6.71	100	13.67	32.57
100	14.37	33.44	135	1.94	16.27
143	2.20	17.21	143	2.18	16.91
146	2.18	16.99	146	2.17	16.83
180	10.42	30.06	181	2.21	17.13
183	2.32	17.19	208	5.66	24.90
223	1.73	11.76	225	6.17	23.43
226	12.33	31.15	227	2.56	17.74
238	6.38	25.42	242	0.90	5.84
258	6.10	25.19	259	10.75	30.92
263	7.86	27.33	264	11.57	30.00
265	4.90	20.87	278	10.43	29.56
279	5.64	24.57	280	3.87	21.18
282	2.01	16.99			

DATA CORRELATION NUMBER 1

THE STANDARD DEVIATION FOR THIS EXPERIMENTAL DATA ABOUT THE CALCULATED CURVE IS 1.5902 FOR A POLYNOMIAL REGRESSION OF ORDER 1.

THE CONSTANTS OF THE CALCULATED POLYNOMIAL ARE:

A=	-5.703
B(1)=	0.5228
B(2)=	0.0
B(3)=	0.0
B(4)=	0.0
B(5)=	0.0

THE CALCULATED MAGNESIUM CONTENTS WHICH FOLLOW WERE CALCULATED USING THE CONSTANTS LISTED ABOVE.

PCT. SI	PCT. MG	PCT. SI	PCT. MG	PCT. SI	PCT. MG
1.0	-5.18	2.0	-4.66	3.0	-4.13
4.0	-3.61	5.0	-3.09	6.0	-2.57
7.0	-2.04	8.0	-1.52	9.0	-1.00
10.0	-0.48	11.0	0.05	12.0	0.57
13.0	1.09	14.0	1.62	15.0	2.14
16.0	2.66	17.0	3.18	18.0	3.71
19.0	4.23	20.0	4.75	21.0	5.28
22.0	5.80	23.0	6.32	24.0	6.84
25.0	7.37	26.0	7.89	27.0	8.41
28.0	8.93	29.0	9.46	30.0	9.98
31.0	10.50	32.0	11.03	33.0	11.55
34.0	12.07	35.0	12.59	36.0	13.12
37.0	13.64	38.0	14.16	39.0	14.69
40.0	15.21				

DATA CORRELATION NUMBER 2

THE STANDARD DEVIATION FOR THIS EXPERIMENTAL DATA ABOUT THE CALCULATED CURVE IS 0.4926 FOR A POLYNOMIAL REGRESSION OF ORDER 2.

THE CONSTANTS OF THE CALCULATED POLYNOMIAL ARE:

A=	3.073
B(1)=	-0.4513
B(2)=	0.02350
B(3)=	0.0
B(4)=	0.0
B(5)=	0.0

THE CALCULATED MAGNESIUM CONTENTS WHICH FOLLOW WERE CALCULATED USING THE CONSTANTS LISTED ABOVE.

PCT. SI	PCT. MG	PCT. SI	PCT. MG	PCT. SI	PCT. MG
1.0	2.65	2.0	2.26	3.0	1.93
4.0	1.64	5.0	1.40	6.0	1.21
7.0	1.07	8.0	0.97	9.0	0.91
10.0	0.91	11.0	0.95	12.0	1.04
13.0	1.18	14.0	1.36	15.0	1.59
16.0	1.87	17.0	2.19	18.0	2.56
19.0	2.98	20.0	3.45	21.0	3.96
22.0	4.52	23.0	5.12	24.0	5.78
25.0	6.48	26.0	7.23	27.0	8.02
28.0	8.86	29.0	9.75	30.0	10.68
31.0	11.67	32.0	12.70	33.0	13.77
34.0	14.90	35.0	16.07	36.0	17.28
37.0	18.55	38.0	19.86	39.0	21.22
40.0	22.62				

DATA CORRELATION NUMBER 3

THE STANDARD DEVIATION FOR THIS EXPERIMENTAL DATA ABOUT THE CALCULATED CURVE IS 0.4746 FOR A POLYNOMIAL REGRESSION OF ORDER 3.

THE CONSTANTS OF THE CALCULATED POLYNOMIAL ARE:

A=	1.367
B(1)=	-0.0912
B(2)=	0.00248
B(3)=	0.000361
B(4)=	0.0
B(5)=	0.0

THE CALCULATED MAGNESIUM CONTENTS WHICH FOLLOW WERE CALCULATED USING THE CONSTANTS LISTED ABOVE.

PCT. SI	PCT. MG	PCT. SI	PCT. MG	PCT. SI	PCT. MG
1.0	1.28	2.0	1.20	3.0	1.13
4.0	1.07	5.0	1.02	6.0	0.99
7.0	0.97	8.0	0.98	9.0	1.01
10.0	1.06	11.0	1.15	12.0	1.25
13.0	1.40	14.0	1.57	15.0	1.78
16.0	2.02	17.0	2.31	18.0	2.64
19.0	3.01	20.0	3.43	21.0	3.89
22.0	4.41	23.0	4.98	24.0	5.60
25.0	6.28	26.0	7.02	27.0	7.83
28.0	8.69	29.0	9.62	30.0	10.62
31.0	11.69	32.0	12.83	33.0	14.04
34.0	15.34	35.0	16.71	36.0	18.16
37.0	19.69	38.0	21.31	39.0	23.02
40.0	24.81				

DATA CORRELATION NUMBER 4

THE STANDARD DEVIATION FOR THIS EXPERIMENTAL DATA ABOUT THE CALCULATED CURVE IS 0.4833 FOR A POLYNOMIAL REGRESSION OF ORDER 4.

THE CONSTANTS OF THE CALCULATED POLYNOMIAL ARE:

A=	-0.047
B(1)=	0.3112
B(2)=	-0.03360
B(3)=	0.001651
B(4)=	-0.0000160
B(5)=	0.0

THE CALCULATED MAGNESIUM CONTENTS WHICH FOLLOW WERE CALCULATED USING THE CONSTANTS LISTED ABOVE.

PCT. SI	PCT. MG	PCT. SI	PCT. MG	PCT. SI	PCT. MG
1.0	0.23	2.0	0.45	3.0	0.63
4.0	0.76	5.0	0.87	6.0	0.95
7.0	1.01	8.0	1.07	9.0	1.13
10.0	1.20	11.0	1.27	12.0	1.37
13.0	1.49	14.0	1.64	15.0	1.82
16.0	2.04	17.0	2.31	18.0	2.62
19.0	2.97	20.0	3.38	21.0	3.85
22.0	4.37	23.0	4.94	24.0	5.58
25.0	6.28	26.0	7.03	27.0	7.85
28.0	8.73	29.0	9.67	30.0	10.66
31.0	11.72	32.0	12.83	33.0	13.99
34.0	15.20	35.0	16.46	36.0	17.77
37.0	19.11	38.0	20.50	39.0	21.91
40.0	23.35				

DATA CORRELATION NUMBER 5

THE STANDARD DEVIATION FOR THIS EXPERIMENTAL DATA ABOUT THE CALCULATED CURVE IS 0.4934 FOR A POLYNOMIAL REGRESSION OF ORDER 5.

THE CONSTANTS OF THE CALCULATED POLYNOMIAL ARE:

A=	-2.747
B(1)=	1.2379
B(2)=	-0.14576
B(3)=	0.007875
B(4)=	-0.0001776
B(5)=	0.00000159

THE CALCULATED MAGNESIUM CONTENTS WHICH FOLLOW WERE CALCULATED USING THE CONSTANTS LISTED ABOVE.

PCT. SI	PCT. MG	PCT. SI	PCT. MG	PCT. SI	PCT. MG
1.0	-1.65	2.0	-0.79	3.0	-0.15
4.0	0.33	5.0	0.68	6.0	0.92
7.0	1.08	8.0	1.18	9.0	1.26
10.0	1.31	11.0	1.37	12.0	1.44
13.0	1.53	14.0	1.66	15.0	1.82
16.0	2.03	17.0	2.29	18.0	2.60
19.0	2.96	20.0	3.38	21.0	3.86
22.0	4.39	23.0	4.97	24.0	5.61
25.0	6.31	26.0	7.06	27.0	7.86
28.0	8.73	29.0	9.65	30.0	10.63
31.0	11.69	32.0	12.81	33.0	14.02
34.0	15.31	35.0	16.71	36.0	18.23
37.0	19.88	38.0	21.68	39.0	23.65
40.0	25.82				

SOLUBILITY DATA ANALYSIS PROGRAM

FOLLOWING ARE THE INPUT AND RESULTS OF A REGRESSION ANALYSIS PROGRAM WHICH ANALYZES SOLUBILITY DATA USING 5 POLYNOMIALS FROM FIRST THROUGH FIFTH ORDER INCLUSIVE

THE RESULTS ARE PRESENTED AS AN EQUATION EXPRESSING THE EQUILIBRIUM MAGNESIUM CONTENT AS A POLYNOMIAL FUNCTION OF SILICON CONTENT.

THE EXPERIMENTAL DATA TO BE ANALYZED FOLLOW:

HEAT	PCT. MG	PCT. SI	HEAT	PCT. MG	PCT. SI
68	53.41	29.58	82	96.70	0.54
135	92.81	4.38	181	91.24	6.10
183	92.60	5.71	207	93.12	4.11
209	93.22	4.65	223	95.80	1.56
278	51.68	30.38	279	71.27	20.47
280	81.10	14.43			

DATA CORRELATION NUMBER 1

THE STANDARD DEVIATION FOR THIS EXPERIMENTAL DATA ABOUT THE CALCULATED CURVE IS 1.9439 FOR A POLYNOMIAL REGRESSION OF ORDER 1.

THE CONSTANTS OF THE CALCULATED POLYNOMIAL ARE:

A=	99.829
B(1)=	-1.5189
B(2)=	0.0
B(3)=	0.0
B(4)=	0.0
B(5)=	0.0

THE CALCULATED MAGNESIUM CONTENTS WHICH FOLLOW WERE CALCULATED USING THE CONSTANTS LISTED ABOVE.

PCT. SI	PCT. MG	PCT. SI	PCT. MG	PCT. SI	PCT. MG
1.0	98.31	2.0	96.79	3.0	95.27
4.0	93.75	5.0	92.23	6.0	90.72
7.0	89.20	8.0	87.68	9.0	86.16
10.0	84.64	11.0	83.12	12.0	81.60
13.0	80.08	14.0	78.56	15.0	77.05
16.0	75.53	17.0	74.01	18.0	72.49
19.0	70.97	20.0	69.45	21.0	67.93
22.0	66.41	23.0	64.89	24.0	63.38
25.0	61.86	26.0	60.34	27.0	58.82
28.0	57.30	29.0	55.78	30.0	54.26
31.0	52.74	32.0	51.22	33.0	49.71
34.0	48.19	35.0	46.67	36.0	45.15
37.0	43.63	38.0	42.11	39.0	40.59
40.0	39.07				

DATA CORRELATION NUMBER 2

THE STANDARD DEVIATION FOR THIS EXPERIMENTAL DATA ABOUT THE CALCULATED CURVE IS 0.3460 FOR A POLYNOMIAL REGRESSION OF ORDER 2.

THE CONSTANTS OF THE CALCULATED POLYNOMIAL ARE:

A=	97.023
B(1)=	-0.7587
B(2)=	-0.02419
B(3)=	0.0
B(4)=	0.0
B(5)=	0.0

THE CALCULATED MAGNESIUM CONTENTS WHICH FOLLOW WERE CALCULATED USING THE CONSTANTS LISTED ABOVE.

PCT. SI	PCT. MG	PCT. SI	PCT. MG	PCT. SI	PCT. MG
1.0	96.24	2.0	95.41	3.0	94.53
4.0	93.60	5.0	92.62	6.0	91.60
7.0	90.53	8.0	89.41	9.0	88.24
10.0	87.02	11.0	85.75	12.0	84.44
13.0	83.07	14.0	81.66	15.0	80.20
16.0	78.69	17.0	77.13	18.0	75.53
19.0	73.88	20.0	72.17	21.0	70.42
22.0	68.63	23.0	66.78	24.0	64.88
25.0	62.94	26.0	60.95	27.0	58.91
28.0	56.82	29.0	54.68	30.0	52.49
31.0	50.26	32.0	47.98	33.0	45.65
34.0	43.27	35.0	40.84	36.0	38.36
37.0	35.84	38.0	33.27	39.0	30.65
40.0	27.98				

DATA CORRELATION NUMBER 3

THE STANDARD DEVIATION FOR THIS EXPERIMENTAL DATA ABOUT THE CALCULATED CURVE IS 0.3696 FOR A POLYNOMIAL REGRESSION OF ORDER 3.

THE CONSTANTS OF THE CALCULATED POLYNOMIAL ARE:

A=	96.997
B(1)=	-0.7472
B(2)=	-0.02518
B(3)=	0.000022
B(4)=	0.0
B(5)=	0.0

THE CALCULATED MAGNESIUM CONTENTS WHICH FOLLOW WERE CALCULATED USING THE CONSTANTS LISTED ABOVE.

PCT. SI	PCT. MG	PCT. SI	PCT. MG	PCT. SI	PCT. MG
1.0	96.22	2.0	95.40	3.0	94.53
4.0	93.61	5.0	92.63	6.0	91.61
7.0	90.54	8.0	89.42	9.0	88.25
10.0	87.03	11.0	85.76	12.0	84.44
13.0	83.07	14.0	81.66	15.0	80.20
16.0	78.68	17.0	77.12	18.0	75.51
19.0	73.86	20.0	72.15	21.0	70.40
22.0	68.60	23.0	66.75	24.0	64.86
25.0	62.91	26.0	60.93	27.0	58.89
28.0	56.81	29.0	54.68	30.0	52.50
31.0	50.28	32.0	48.01	33.0	45.69
34.0	43.33	35.0	40.92	36.0	38.47
37.0	35.97	38.0	33.42	39.0	30.83
40.0	28.20				

DATA CORRELATION NUMBER 4

THE STANDARD DEVIATION FOR THIS EXPERIMENTAL DATA ABOUT THE CALCULATED CURVE IS 0.3918 FOR A POLYNOMIAL REGRESSION OF ORDER 4.

THE CONSTANTS OF THE CALCULATED POLYNOMIAL ARE:

A=	97.094
B(1)=	-0.8336
B(2)=	-0.00818
B(3)=	-0.000990
B(4)=	0.0000179
B(5)=	0.0

THE CALCULATED MAGNESIUM CONTENTS WHICH FOLLOW WERE CALCULATED USING THE CONSTANTS LISTED ABOVE.

PCT. SI	PCT. MG	PCT. SI	PCT. MG	PCT. SI	PCT. MG
1.0	96.25	2.0	95.39	3.0	94.49
4.0	93.57	5.0	92.61	6.0	91.61
7.0	90.56	8.0	89.47	9.0	88.33
10.0	87.13	11.0	85.88	12.0	84.57
13.0	83.21	14.0	81.79	15.0	80.31
16.0	78.78	17.0	77.19	18.0	75.55
19.0	73.85	20.0	72.10	21.0	70.30
22.0	68.45	23.0	66.56	24.0	64.63
25.0	62.67	26.0	60.67	27.0	58.66
28.0	56.62	29.0	54.56	30.0	52.50
31.0	50.44	32.0	48.38	33.0	46.34
34.0	44.32	35.0	42.33	36.0	40.38
37.0	38.48	38.0	36.63	39.0	34.86
40.0	33.16				

DATA CORRELATION NUMBER 5

THE STANDARD DEVIATION FOR THIS EXPERIMENTAL DATA ABOUT THE CALCULATED CURVE IS 0.4195 FOR A POLYNOMIAL REGRESSION OF ORDER 5.

THE CONSTANTS OF THE CALCULATED POLYNOMIAL ARE:

A=	97.241
B(1)=	-1.0344
B(2)=	0.04892
B(3)=	-0.006614
B(4)=	0.0002420
B(5)=	-0.00000309

THE CALCULATED MAGNESIUM CONTENTS WHICH FOLLOW WERE CALCULATED USING THE CONSTANTS LISTED ABOVE.

PCT. SI	PCT. MG	PCT. SI	PCT. MG	PCT. SI	PCT. MG
1.0	96.25	2.0	95.32	3.0	94.42
4.0	93.52	5.0	92.61	6.0	91.66
7.0	90.66	8.0	89.60	9.0	88.48
10.0	87.29	11.0	86.02	12.0	84.69
13.0	83.29	14.0	81.83	15.0	80.31
16.0	78.74	17.0	77.12	18.0	75.46
19.0	73.76	20.0	72.03	21.0	70.27
22.0	68.49	23.0	66.67	24.0	64.82
25.0	62.94	26.0	61.01	27.0	59.02
28.0	56.96	29.0	54.80	30.0	52.52
31.0	50.09	32.0	47.48	33.0	44.64
34.0	41.52	35.0	38.09	36.0	34.26
37.0	29.98	38.0	25.17	39.0	19.75
40.0	13.63				

BIBLIOGRAPHY

1. Tesman, A. B., "How the Russians Make and Use Nodular Iron," Metals Progress, 90, Sept. 1966, p. 111.

2. Barnum, H. "Theories and Methods of Excitement to Produce Ductile Iron," Bulletin No. 41, Ductile Iron Society, 1966, p. 35.

3. White, R. W. "Magnesium Treatment Techniques," Journal of Metals, 12, June, 1960, p. 464-466.

4. Clark, R. A. and T. K. McCluhan, "Influence of Magnesium Content on the Nodularizing Efficiency of Magnesium-Ferrosilicon Alloys," Trans. AFS, 73, 1965, p. 242.

5. Hansen, M. Constitution of Binary Alloys, McGraw-Hill, 1958.

6. Chipman, J., Fulton, J. C., Gockcen, N., and G. R. Caskey, "Activity of Silicon in Liquid Fe-Si and Fe-C-Si Alloys," ACTA Met., 2, 1954, p. 439.

7. Darken, L. S. and R. W. Gurry, Physicial Chemistry of Metals, McGraw-Hill, 1953, p. 254.

8. Eldridge, J. M., Miller, E., and K. L. Komarek, "Thermodynamic Properties of Liquid Magnesium-Silicon Alloys. Discussion of the Mg-Group IV B Systems," Trans. AIME, 239, 1967, p. 775.

9. Trojan, P. K., Liquid-Liquid Equilibria and Thermodynamic Data for the Fe-C-Si-Mg System, Ph.D. Dissertation, The University of Michigan, Ann Arbor, Michigan, 1961.

10. Sponseller, D. L., Third Element Interactions with the System Liquid Iron-Liquid Calcium, Ph.D. Dissertation, The University of Michigan, Ann Arbor, Michigan, 1962.

11. Zwicker, V., "Reactions Between Some Magnesium Alloys and Liquid Cast Iron," Z. Metallkunde, 45, 1954, p. 31.

12. Klodt, D. T., A Study of the Factors Controlling Immiscibility in Liquid-Metal Alloys, Report #2458, Denver Research Institute, 1968.

13. Case, L. O., Elements of the Phase Rule, The Edwards Letter Shop, Ann Arbor, Michigan (1939).

14. Smith, D. P., "Fundamental Metallurgical and Thermodynamic Principles of Gas-Metal Behavior," Gases in Metals, A.S.M. (1953), p. 16.

15. Chipman, J., "Physical Chemistry of High-Temperature Reactions," Basic Open Hearth Steelmaking, AIME (1964), p. 580.

16. Nesmeyanov, A. N., Vapor Pressures of the Chemical Elements, Elsevier, 1963.

17. Hartmann, H. and R. Schneider, "The Boiling Temperatures of Magnesium, Calcium, Strontium, Barium and Lithium," Z. Anorg. Chem., 180, 1929, p. 275.

18. Hultgren, R., Orr, R. L., Anderson, P. D. and K. K. Kelly, Selected Values of Thermodynamic Properties of Metals and Alloys, John Wiley and Sons, 1963.

19. Greenbank, J. C. and B. B. Argent, "Vapor Pressure of Magnesium, Zinc and Cadmium," Trans. Far. Soc., 61, 1965, p. 655.

20. Barto, R. L. and D. T. Hurd, "Refractory Metals in Liquid Metals Handling," Research/Development, Nov. 1966, p. 28.

21. Chiotti, P., Tracy, G. A., and H. A. Wilhelm, "Magnesium-Uranium System," Trans. AIME, 206, 1956, p. 562.

22. Chiotti, P., Ames Laboratory, Iowa State University, Ames, Iowa (private communication).

23. Coleman, F. F., and A. C. Egerton, Phil. Trans. 234, 1934-1935, p. 177.

24. Vetter, F. A. and O. Kubaschewski, Z. Electrochem, 57, 1953, p. 243.

25. Priselkov, Yu. A., Vapor Pressure Measurement, Dissertation, Moscow State University, Moscow, 1954.

26. Findlay, A., A. N. Campbell, and N. O. Smith, The Phase Rule, 9th ed., Dover 1951, p. 285.

27. Robertson, J. C. and W. R. Von Tress, "Factors Affecting Magnesium Absorption in Molten Iron," Bulletin No. 42, Ductile Iron Society, 1966, p. 27.

28. Grandpierre, M. C. M., U. S. Patent 2,781,260, Feb., 1957.

29. Trojan, P. K., and R. A. Flinn, "Fundamentals of Magnesium Addition to Ductile Iron," Trans. SAE, 73, 1965, p. 265.

30. R. A. Clark, Union Carbide Corporation (private communication).